GEOSTANDARDS and GEOANALYTICAL RESEARCH

ND70 Series Basaltic Glass Reference Materials for Volatile Element (H_2O, CO_2, S, Cl, F) Measurement and the C Ionisation Efficiency Suppression Effect of Water in Silicate Glasses in SIMS

Yves **Moussallam** (1)*, William Henry **Towbin** (2), Terry **Plank** (1), Hélène **Bureau** (3), Hicham **Khodja** (4), Yunbin **Guan** (5), Chi **Ma** (5), Michael B. **Baker** (5), Edward M. **Stolper** (5), Fabian U. **Naab** (6), Brian D. **Monteleone** (7), Glenn A. **Gaetani** (7), Kenji **Shimizu** (8), Takayuki **Ushikubo** (8), Hyun Joo **Lee** (1), Shuo **Ding** (1), Sarah **Shi** (1) and Estelle F. **Rose-Koga** (9)

(1) Lamont-Doherty Earth Observatory, Columbia University, New York, USA
(2) Gemological Institute of America, 50 W. 47th Street, New York, NY 10036, United States of America
(3) IMPMC, Sorbonne Université, CNRS UMR 7590, MNHN, IRD UR 206, 4 place Jussieu, 75252 Paris Cedex 05, France
(4) LEEL, NIMBE, CEA, CNRS, Université Paris-Saclay, CEA Saclay, 91191 Gif sur Yvette Cedex, France
(5) Division of Geological and Planetary Sciences, California Institute of Technology, Pasadena, California 91125, USA
(6) Department of Nuclear Engineering and Radiological Sciences, University of Michigan, Ann Arbor, Michigan 48109, USA
(7) Department of Geology and Geophysics, Woods Hole Oceanographic Institution, Woods Hole, MA 02543, USA
(8) Kochi Institute for Core Sample Research, X-star, Japan Agency for Marine-Earth Science and Technology, Monobe-otsu 200, Nankoku, Kochi 783-8502, Japan
(9) ISTO, UMR 7327, CNRS-UO-BRGM, 1A rue de la Férollerie, 45071 Orléans cedex 2, France
* Corresponding author. e-mail: yves.moussallam@ldeo.columbia.edu

We present a new set of reference materials, the ND70-series, for *in situ* measurement of volatile elements (H_2O, CO_2, S, Cl, F) in silicate glass of basaltic composition. The materials were synthesised in piston cylinders at pressures of 1 to 1.5 GPa under volatile-undersaturated conditions. They span mass fractions from 0 to 6% *m/m* H_2O, from 0 to 1.6% *m/m* CO_2 and from 0 to 1% *m/m* S, Cl and F. The materials were characterised by elastic recoil detection analysis for H_2O, by nuclear reaction analysis for CO_2, by elemental analyser for CO_2, by Fourier transform infrared spectroscopy for H_2O and CO_2, by secondary ion mass spectrometry for H_2O, CO_2, S, Cl and F, and by electron probe microanalysis for CO_2, S, Cl and major elements. Comparison between expected and measured volatile amounts across techniques and institutions is excellent. It was found however that SIMS measurements of CO_2 mass fractions using either Cs^+ or O^- primary beams are strongly affected by the glass H_2O content. Reference materials have been made available to users at ion probe facilities in the US, Europe and Japan. Remaining reference materials are preserved at the Smithsonian National Museum of Natural History where they are freely available on loan to any researcher.

Keywords: reference materials, volatiles, silicate melts, SIMS, ERDA, NRA, FTIR, EPMA.

Received 26 Feb 24 – Accepted 21 May 24

Volatile elements (C-O-H-S-Cl-F) play a major role in planetary processes including habitability (e.g., Ehlmann *et al.* 2016, Foley and Smye 2018, Dehant *et al.* 2019), plate tectonics (e.g., Albarède 2009, Stern 2018, Nicoli and Ferrero 2021), mantle melting (e.g., Wyllie 1971, Eggler 1976, Dasgupta and Hirschmann 2006) and volcanic eruptions (e.g., Elskens *et al.* 1968, Allard 2010, Edmonds and Woods 2018). Understanding the planetary-scale cycling of volatiles has hence long been a subject of interest to geoscientists. Critical to that effort is the ability to reliably measure volatiles in geological materials. For volcanologists, igneous petrologists and mantle geochemists, the ability to measure volatile elements in melts (i.e., glasses) and mineral-hosted melt inclusions is of particular

doi: 10.1111/ggr.12572

interest (e.g., Dixon et al. 1988, Hauri et al. 2002, Métrich and Wallace 2008). Secondary Ion Mass Spectrometry (SIMS) is a technique that allows for the measurements of all major volatile species in silicate glasses (e.g., Shimizu et al. 2017). One persistent issue with SIMS analyses however is that the ionisation efficiency varies by element, primary beam, and major element matrix. To be fully quantitative, the technique requires well-characterised reference materials with bulk compositions similar to that of the sample. To date, ion microprobe facilities in Nancy, Paris, Lausanne, Edinburgh, Washington, Woods Hole, Pasadena, Tempe and Kochi, amongst other, have all either acquired or synthesised their own sets of reference material for volatile elements in basaltic glasses. Although sharing natural reference materials is quite common (e.g., Shimizu et al. 2017), efforts to synthesise large amounts of glasses and to cross-calibrate instruments prior to using the synthetic glasses as reference materials have been quite limited, particularly on an international scale. This has resulted in significant challenges when attempting to directly compare measurement results generated by different facilities. Furthermore, not all of these facilities possess reference materials that span the entire range of volatile mass fractions found in geological samples. As a consequence, some measurements rely on extrapolation from calibration curves. In this context, we introduce and thoroughly characterise a new series of synthetic basaltic glasses. These glasses are intended to serve as international reference materials for the analysis of H_2O, CO_2, S, Cl, and F mass fractions in natural glasses with a basaltic composition, particularly in the context of SIMS and other micro-beam techniques.

Experimental method

We used as starting material a natural Back-Arc-Basin-Basalt, ND-70, dredged at Latitude 15° 52′ S, Longitude 174°51′ W from a depth of 2500 m below sea level (Keller et al. 2008) at the Mangatolu Triple Junction in the northern Lau back-arc region (initial composition: 49.2% *m/m* SiO_2, 0.8% *m/m* TiO_2, 16.1% *m/m* Al_2O_3, 7.9% *m/m* FeO_{tot}, 8.2% *m/m* MgO, 12.8% m/m CaO, 1.9% *m/m* Na_2O, 0.15% m/m K_2O, 0.1% *m/m* P_2O_5, 889 µg g^{-1} S, 219 µg g^{-1} Cl, 1.02% *m/m* H_2O, 76 µg g^{-1} CO_2, and 148 µg g^{-1} F, Keller et al. 2008, Caulfield et al. 2012, Lloyd et al. 2013). Five grams of material were crushed, placed in a platinum crucible and fused at 0.1 MPa, in air, at 1350 °C for 2 h, quenched in water (without submersing the crucible), crushed and mixed again and fused a second time at 1350 °C, 0.1 MPa, in air, for an additional two hours and quenched again in water (without submersing the crucible). This volatile-free glass (ND70-degassed) constituted the first sample in our reference material suite (i.e., the blank), and was then used as the starting powder for subsequent piston cylinder experiments.

High-pressure experiments were prepared by adding powdered ND70-degassed glass with the desired amounts of H_2O, CO_2, S, Cl and F in $Au_{80}Pd_{20}$ capsules, which were then welded shut. H_2O was loaded as de-ionised water (using a micro-pipette), CO_2 was loaded as powdered calcite ($CaCO_3$), S was loaded as anhydrite ($CaSO_4$), Cl was loaded as halite (NaCl) and F was loaded as sellaite (MgF_2). Table 1 gives the intended composition of each experiment based on the added mass of each component (given in online supporting information Table S1 and totalling 150 to 200 mg per experiment). High-pressure experiments were all performed in a piston cylinder apparatus at the Lamont-Doherty Earth Observatory (LDEO). We used a 1/2-inch assembly composed of a CaF_2 pressure cell, a graphite furnace, and MgO sleeves and spacers surrounding the ($\varnothing_{ext}$ = 5.0 mm, $\varnothing_{int}$ = 4.8 mm, length = 8.0 mm) $Au_{80}Pd_{20}$ capsule. The temperature was monitored with a D-type ($W_{97}Re_3$-$W_{75}Re_{25}$) thermocouple, separated from the capsule by a 0.8 mm alumina disc. No attempt at controlling oxygen fugacity was made, although given that our starting powder (ND70-degassed) was fused in air, we assume highly oxidised conditions. Run conditions for each experiment are reported in Table 2. Piston cylinder experiments were conducted at pressures of 1 and 1.5 GPa, temperatures of 1225 and 1325 °C and equilibrated for 2 h. Experiments were quenched by turning off the electric power and took approximately 5 s to cool bellow 400 °C. An additional experiment, INSOL_MX1_BA4, was run using a powdered mixture of natural basalt (60%) and dacite (30%) (from Kilauea and Tutupaca volcanoes, respectively, Moussallam et al. unpublished) with dolomite (10%) following the same piston cylinder methodology as described above and equilibrated at 1 GPa and 1275 °C for 2 h. No additional water, S, Cl nor F was added. Initial CO_2 was far above saturation. Finally another experiment VILLA_P2 was run using a powdered mixture of natural basaltic andesite from Villarrica volcano (same starting material as described in Moussallam et al. 2023) to which de-ionised water, elemental sulfur and oxalic acid dihydrate were added such that the initial mass fractions of CO_2 and S would be above saturation level (based on previous experiments on similar compositions) at the conditions of the experiment. The charge was run in an internally heated pressure vessel at the American Museum of Natural History and equilibrated at 300 MPa, 1150 °C for 2 h at the intrinsic fO_2 of the vessel (~ NNO+2; Webster et al. 2011). Both INSOL_MX1_BA4 and VILLA_P2 are not part of the reference material suite that we present here as they were not synthesised in sufficient quantities but were used for calibration purposes during

Table 1.
Expected chemical composition (in % *m/m* unless otherwise indicated) of all experiments based on loaded amounts of starting material

Sample name	SiO_2	TiO_2	Al_2O_3	FeO_{tot}	MnO	MgO	CaO	Na_2O	K_2O	P_2O_5	H_2O	CO_2 (µg g^{-1})	S (µg g^{-1})	Cl (µg g^{-1})	F (µg g^{-1})	Total
ND 70_ Degassed	50.18	0.85	16.54	8.18	0.17	8.44	13.18	2.21	0.17	0.09	0.00	0	0	0	0	100
ND70-2-01	48.74	0.82	16.06	7.95	0.17	8.28	13.01	2.20	0.17	0.08	2.25	665	672	679	717	100
ND70-3-01	48.15	0.81	15.87	7.85	0.16	8.21	12.95	2.21	0.16	0.08	3.13	989	1001	1011	1067	100
ND70-4-01	47.26	0.80	15.58	7.71	0.16	8.18	13.01	2.26	0.16	0.08	3.99	1970	1993	2013	2125	100
ND70-4-02	47.15	0.80	15.54	7.69	0.16	8.16	12.98	2.25	0.16	0.08	4.22	1965	1988	2008	2120	100
ND70-5-02	47.27	0.71	13.88	6.87	0.14	7.67	13.27	2.33	0.14	0.07	5.01	10349	5072	5468	5497	100
ND70-5-03	48.17	0.81	15.88	7.85	0.16	8.13	12.71	2.14	0.16	0.08	3.82	197	200	202	213	100
ND70-6-02	44.29	0.67	13.01	6.43	0.13	7.71	14.06	2.64	0.13	0.07	6.28	15023	10177	10363	10112	100

Table 2.
Experimental conditions

Experiment #	Pressure (MPa)	Temperature (°C)	Duration (h)
ND 70_ Degassed	0.1	1350	4
ND70-2-01	1000	1325	2
ND70-3-01	1000	1325	2
ND70-4-01	1000	1225	2
ND70-4-02	1000	1325	2
ND70-5-02	1500	1325	2
ND70-5-03	1500	1325	2
ND70-6-02	1500	1325	2

some of the SIMS sessions discussed below. All samples were entirely glassy except ND70-4-01, which partially crystallised on one side of the capsule (the partially crystallised portion was mechanically removed).

Analytical techniques

Experiments were performed by Elastic Recoil Detection Analysis (ERDA) for H_2O, by Nuclear Reaction Analysis (NRA) for CO_2, by Elemental Analyser (EA) for CO_2, by Fourier Transform Infrared Spectroscopy (FTIR) for H_2O and CO_2, by Secondary Ion Mass Spectrometry (SIMS) for H_2O, CO_2, S, Cl and F, and by Electron probe microanalyser (EPMA) for CO_2, S, Cl and major elements.

Nuclear microprobe (ERDA and NRA)

H_2O and CO_2 absolute mass fractions were evaluated using two ion beam analysis techniques, namely Elastic Recoil Detection Analysis (ERDA) and Nuclear Reaction Analysis (NRA). Measurements were performed at the Laboratoire d'Etude des Eléments Légers (LEEL) joint CEA-CNRS laboratory in Saclay (Khodja *et al.* 2001) where these techniques are regularly employed to quantify low atomic number elements in various materials, including geological samples (Clesi *et al.* 2018, Malavergne *et al.* 2019). H_2O was measured as H by ERDA following the approaches described in Bureau *et al.* (2009). We used a $^4He^+$ ion beam at 2.7 MeV energy that interacted with the samples at grazing incidence. A 12-µm Mylar absorber was mounted between the sample and the forward (30°) particle detector to stop all scattered $^4He^+$ and let recoil H^+ ions reach the detector. The CO_2 was measured as C by NRA, making use of the sensitive $^{12}C(d,p)^{13}C$ nuclear reaction at 170° detection angle using a deuteron ($^2H^+$) microbeam at 1.4 MeV. Although no absorber was used, detected protons, in the 2750–3150 keV energy range, are far above backscattered deuterons. Quantification was performed by precisely measuring detector solid angles using reference materials and by adjusting experimental spectra with the SIMNRA software (Mayer 1999). The parasitic contribution from the $^{28}Si(d,p)^{29}Si$ was systematically subtracted using a Suprasil reference spectrum ($H_2O < 1$ µg g^{-1}, e.g., Shimizu *et al.* 2019).

Elemental analyser

A Costech elemental analyser (ECS4010) at the Lamont-Doherty Earth Observatory was used to measure CO_2 (as C) in the two most CO_2-rich experiments (with > 1% *m/m* CO_2). Handpicked glass samples were precisely weighed on a microbalance with a precision of ± 0.001 mg, and then wrapped in 3.2 × 4 mm tin foil envelopes. 18.253 mg were used for sample ND70-5-02 and 12.636 mg were used for sample ND70-6-02. These encapsulated samples were subjected to combustion (at ~ 1700 °C) over a chromium (III) oxide catalyst with excess oxygen (25 ml min^{-1}). The carrier gas was helium, flowing at a rate of 100 ml min^{-1}. To ensure complete oxidation of sample carbon into CO_2 and the elimination of remaining halogens or sulfur, silvered cobaltous/cobaltic oxide, positioned lower in the quartz combustion tube, was used. The analyser was calibrated directly prior to sample analysis using mixtures of oxalic acid and SiO_2 with 1, 2, 5, 20 and 70% *m/m* of CO_2. This calibration (R^2 = 0.9999, online supporting information Figure S1) was then used to determine the CO_2 content of the samples. Error on C was estimated at ± 2% (± 7.3% on CO_2) based on reproducibility of external reference materials (calcite and dolomite) similar to other studies using an elemental analyser for silicate glasses (e.g., Moussallam *et al.* 2015, 2016).

Fourier transform infrared spectroscopy (FTIR)

H_2O and CO_2 mass fractions in doubly polished experimental glasses were measured using a N_2 purged Thermo Scientific Nicolet iN10 mx Fourier Transform Infrared Spectrometer (FTIR) at LDEO. Measurements were collected with aperture sizes varying between 100 × 100 µm and 200 × 200 µm. Thickness of the doubly polished wafers were measured using a digital micrometer (Mitutoyo Digimatic Indicator) and calculated using the "interference fringe" method (Tamic *et al.* 2001) that requires determining the wavelength of interference fringes of reflectance spectra collected from the sample. The latter method enables determining the thickness at the same spot where the transmission spectra is collected. Several spots were measured on each glass to ensure no heterogeneity. Baseline fitting, density calculations, absorption coefficients and ultimately H_2O and CO_2 concentration were determined using PyIRoGlass (Shi *et al.* 2023, https://github.com/sarahshi/PyIRoGlass), except for INSOL_MX1_BA4 where we used the spectra obtained from a de-volatised (i.e., fused twice at 0.1 MPa in air for 2 h) version of the same composition to define the baseline.

Secondary ion mass spectrometry at CRPG-CNRS (Nancy)

A first indium mount containing all the experimental glasses was cleaned with DI and Millipore filtered water, dried and then coated with a ~ 20 nm Au layer. Volatile (H_2O, CO_2, Cl, F, S) contents in experimental glasses were determined using a Cameca IMS 1280 ion microprobe at CRPG-CNRS-Nancy, France. A 20 kV (10 kV for the ion acceleration at the source and 10 kV for ion extraction at the sample surface) Cs^+ primary beam was used with a current of 1 nA. A -10 kV electron flood gun was applied at the sample surface to charge compensate the positive Cs^+ ion surface implantation. During analysis (with e-gun on), the sample potential was held at -5 kV and the electron gun was operated at -5 kV, so that electrons arrive at the sample surface with near-zero energy. A 180 s pre-sputter with a 30 µm × 30 µm square raster was applied, then measurements were collected on the 15 to 20 µm spot in the centre of the rastered area using a mechanical aperture placed at the secondary ion image plane. Analyses were performed in multi-collector mode; CO_2, H_2O, F, Cl and S were measured using an electron multiplier, while Si and O were measured on a Faraday cup. We collected signals for ^{12}C (8 s), ^{17}O (3 s), $^{16}O^1H$ (6 s), ^{18}O (3 s), ^{19}F (4 s), ^{27}Al (3 s), ^{30}Si (3 s), ^{32}S (4 s) and ^{35}Cl (6 s; counting times in parentheses), with 2 s waiting time after each switch of the magnet. This cycle was repeated ten times during one analysis for a total analysis duration of 12 min. The mass resolution of ~ 7000 (with the contrast aperture at 400 µm, the energy aperture at 40 eV, the entrance slit at 52 µm and the exit slit at 173 µm) meant that complete discrimination of the following mass interferences was achieved: $^{34}S^1H$ on ^{35}Cl; ^{17}O on $^{16}O^1H$; $^{29}Si^1H$ on ^{30}Si; $^{31}P^1H$ on ^{32}S.

Together with our experimental glasses, we measured natural and experimental basaltic glasses KL2G (Jochum *et al.* 2006) KE12 (Mosbah *et al.* 1991), VG2 (Jarosewich *et al.* 1980), experimental glasses N72, M34, M35, M40, M43 and M48 (Shishkina *et al.* 2010), and the Macquarie glasses 40428 and 47963 (Kamenetsky *et al.* 2000) under the same analytical conditions at the beginning and end of the session. The calibration lines are shown in Figures S2 to S6. All existing reference material values are reported in Table S2.

Secondary ion mass spectrometry at Woods Hole Oceanographic Institution

A second indium mount containing a different set of chips of the experimental glasses, was cleaned with DI and Millipore filtered water, dried and then coated with a ~ 20 nm Au layer. Volatile concentration analyses were conducted on a Cameca IMS1280 at the Northeast National Ion Microprobe Facility (NENIMF) at the Woods Hole Oceanographic Institution. The reference materials were measured in separate sessions using a $^{133}Cs^+$ primary beam, then a $^{16}O^-$ primary beam. The calibration lines are shown in Figures S2 to S7.

Cs SIMS measurements: A 500 pA to 1 nA $^{133}Cs^+$ primary ion beam, accelerated 10 kV, was focused to a 10–15 µm diameter, then rastered to produce a ~ 25 µm × 25 µm crater. Secondary ions ($^{12}C^-$, $^{16}OH^-$, $^{18}O^-$, $^{19}F^-$, $^{30}Si^-$, $^{31}P^-$, $^{32}S^-$ and $^{35}Cl^-$) were extracted with a 10 kV voltage potential.

The extracted and magnified secondary ions were centred through a 600 μm × 600 μm mechanical field aperture, which blocked transmission of secondary ions from outside of the central ~ 7.5 × 7.5 μm^2 of the crater. The secondary field aperture is necessary to minimise the transmission of background and surficial volatile ions residing in the sample chamber, the surrounding sample surface, and within the outer edges of the sputtered crater. A normal-incidence electron gun set at -10 kV was used to compensate for positive charge build up within the sample crater. The energy bandwidth for the secondary ions was ~ 60 eV. A mass resolving power > 5500 was used to separate interfering masses, such as $^{17}O^-$ from $^{16}OH^-$. Each measurement consisted of 180 s of pre-sputtering, automatic secondary beam centring, and automatic mass calibration, followed by five cycles of counting of each ion intensity on an ETP electron multiplier in magnet peak jumping mode. Count times in seconds for each mass were as follows: $^{12}C^-$ = 10, $^{16}OH^-$ = 5, $^{18}O^-$ = 3, $^{19}F^-$ = 5, $^{30}Si^-$ = 3, $^{31}P^-$ = 5, $^{32}S^-$ = 5, $^{35}Cl^-$ = 5. Background intensities were measured on Suprasil 3002 glass for C, OH, F, P and S, and on Herasil glass for Cl.

O^- SIMS measurements: A 10 nA $^{16}O^-$ primary ion beam, accelerated 13 kV, was focused to a ~ 25 μm diameter, then rastered to produce a ~ 30 to 35 μm diameter crater. Secondary ions ($^{12}C^+$, $^{16}O^+$, $^{16}OH^+$, $^{19}F^+$, $^{30}Si^+$, $^{31}P^+$, $^{32}S^+$ and $^{35}Cl^+$) were extracted with a 10 kV voltage potential. A 1250 μm × 1250 μm mechanical field aperture was set to blocked transmission of secondary ions from outside of the central ~ 15 μm × 15 μm the measurement crater. The energy bandwidth for the secondary ions was ~ 50 eV. A mass resolving power > 5500 was used to separate interfering masses, such as $^{17}O^+$ from $^{16}OH^+$. Each measurement consisted of 120 s of pre-sputtering, automatic secondary beam centring, and automatic mass calibration, followed by five cycles of counting of each ion intensity on an ETP electron multiplier in magnet peak jumping mode. Count times in seconds for each mass were as follows: $^{12}C^+$ = 5, $^{16}O^+$ = 3, $^{16}OH^+$ = 5, $^{19}F^+$ = 5, $^{30}Si^-$ = 2, $^{31}P^+$ = 5, $^{32}S^+$ = 5, $^{35}Cl^+$ = 5. Background intensities were measured on Suprasil 3002 glass for C, OH, F, P and S, and on Herasil glass for Cl.

Secondary ion mass spectrometry at Caltech

Volatile mass fractions measurements were conducted on a Cameca ims-7f GEO instrument at the Caltech Microanalysis Center on the second indium mount. The reference materials were first measured with a Cs^+ beam, and later with a $^{16}O^-$ beam. The calibration lines are shown in Figures S2 to S7.

Cs^+ SIMS measurements: A 10 kV Cs^+ primary ion beam of ~ 3–4 nA (~ 15 μm in diameter) was used to sputter the samples and produce secondary ions. The beam was rastered to produce craters ~ 25 μm × 25 μm in dimension, and a 100 μm field aperture was used to enable only the ions from the central 8 μm of the craters to be transmitted for detection. Possible edge effects were further eliminated with electronic gating (36% in area). Secondary ions ($^{12}C^-$, $^{16}OH^-$, $^{18}O^-$, $^{19}F^-$, $^{30}Si^-$, $^{31}P^-$, $^{32}S^-$ and $^{35}Cl^-$) of -9 keV were collected with an electron multiplier (EM) in the peak-jumping mode. Each measurement consisted of 120 s pre-sputtering, followed by automated secondary beam alignment, peak centring, and 20 cycles of data collection. The counting time of each mass was 1 s per cycle. The energy bandwidth for the secondary ions was set at ~ 45 eV. Sample charging compensation was provided by a normal-incidence electron gun NEG at -9 kV. A mass resolving power (MRP) of ~ 5000 was used to remove any significant interferences to the masses of interest (e.g., $^{17}O^-$ from the $^{16}OH^-$ peak). Data were corrected for EM background and dead time. The instrumental volatile backgrounds were checked with the Suprasil 3002 glass.

O^- SIMS measurements: For this SIMS set-up, a focused $^{16}O^-$ primary beam of -13 kV and ~ 8 nA was used to sputter areas of 25 mm × 25 mm for analysis. Positive secondary ions of $^1H^+$, $^{12}C^+$, and $^{28}Si^+$ of +8.5 kV were collected in the peak-jumping mode with an EM (for $^1H^+$, $^{12}C^+$) or a Faraday cup (FC, for $^{28}Si^+$). Each measurement consisted of twenty cycles of counting of $^1H^+$ (1 s), $^{12}C^+$ (3 s), and $^{28}Si^+$ (1 s). Because there were no significant interferences to the masses of interest, the mass spectrometer was operated at low mass resolution conditions (MRP ~ 1800). Minimal sample charging was corrected with automatic scan and adjustment of the sample high voltage during measurement. The other analytical parameters and operation were similar to those used for the Cs^+ session. The C and H backgrounds were checked with Suprasil for this O^- session, which yielded $^1H^+/^{28}Si^+$ = 3.7E-5 and $^{12}C^+/^{28}Si^+$ = 2.1E-7. Such backgrounds were insignificant to the measured CO_2 and H_2O concentrations in this set of reference materials. Nevertheless, the reported results were corrected for this background.

Secondary ion mass spectrometry at JAMSTEC-Kochi

All the experimental glasses were polished and embedded in a third, indium-filled aluminium disc together with an internal reference material basaltic glass of EPR-G3. After cleaning by acetone and de-ionised water, the sample mount was dried in a vacuum oven for a day and then coated with ~30 nm Au. Volatile (H_2O, CO_2, Cl, F, S) contents in the experimental glasses were determined using a Cameca IMS 1280 ion microprobe at the Kochi Institute, JAMSTEC, Japan, following the method of Shimizu *et al.* (2017). We used a 10 to 15 μm diameter Cs^+ primary beam with a current of ~0.5 nA and an electron gun to compensate for charge build-up at the sample surface. The field aperture size was set at 1 mm × 1 mm corresponding to 5 μm × 5 μm of the field of view of the secondary ion image in order to collect signals from the centre of the analysis spot to avoid surface contamination near the beam edge. Mass resolving power of ~6000 was applied for separating interference signals. Analyses were performed by a magnetic peak switching method. Secondary ion signals of ^{12}C (3 s counting time), ^{16}OH (1 s), ^{19}F (1 s), ^{30}Si (1 s), ^{31}P (1 s), ^{32}S (1 s) and ^{35}Cl (1 s) were detected by an axial electron multiplier (there was a 2-s waiting time after each switch of the magnet). Each analysis consisted of 20 s for pre-sputtering, 120 s for auto-centring of secondary ions to the field and contrast apertures and ten cycles of measurements. The total measurement duration for each analysis was ~7 min. To evaluate the volatile contents of the experimental glasses, we used in-house synthetic and natural silicate glass reference materials described in Shimizu *et al.* (2017). The volatile contents of these in-house reference materials were determined by FTIR (H_2O and CO_2 contents) and pyrohydrolysis-ion chromatography (F, Cl and S contents) (Shimizu *et al.* 2015). Calibration lines are shown in Figures S2 to S7.

EPMA at Caltech

Carbon contents of the glass samples ND70-3-01, ND70-4-02, ND70-5-02 and ND70-6-02, as well as the following secondary reference materials (five gem-quality scapolites (from Prof. George Rossman), a natural spurrite (from the Caltech mineral collection; CIT-11435, Joesten 1974), and a eutectic glass composition in the $CaO-Al_2O_3-SiO_2$ (CAS) system) were analysed at Caltech using a JEOL JXA-iHP200F field-emission electron microprobe in WDS mode, interfaced with the *Probe for EPMA* software from Probe Software, Inc. The secondary reference materials were carefully polished to a ¼ μm finish and treated ultrasonically in ethanol; the scapolites were mounted in indium while the spurrite and CAS glass were mounted in epoxy (the ND-series glasses were prepared at Lamont). Just prior to the start of the measurement session, the ND-series glasses, secondary reference materials, and primary reference materials were plasma cleaned using an Evactron system to remove hydrocarbon contamination on their surfaces and then coated with an ~1-nm layer of Ir (Armstrong and Crispin 2013) using a Cressington 208HR sputter coater (all samples were coated at the same time). Analytical conditions were 10 kV and 15 kV accelerating voltages, a 50 nA beam current, and a 10 μm defocused beam. The LDE2 crystal was used for carbon analysis and counting times were 60 s on peak and 30 s on each background. The on-peak O interference with the C peak, revealed by WDS scans of the glass samples, was corrected using the *Probe for EPMA* program. Cohenite (Fe_3C, *CKα*) from the iron meteorite Canyon Diablo and Elba hematite (*OKα*; for the C on-peak interference correction) were used as primary reference materials. Each ND-series glass and secondary reference material was analysed five times. Quantitative carbon analyses were processed with the CITZAF matrix correction procedure (Armstrong 1995) using the major and minor element composition of each phase.

For the secondary reference materials, the CO_2 contents of the five gem-quality scapolites were determined using NRA at the Michigan Ion Beam Laboratory at the University of Michigan using a deuteron beam energy of 1.35 MeV and procedures described in Hammerli *et al.* (2021). The measured CO_2 contents ranged from 0.70 to 3.57% *m/m*. The CAS eutectic glass was fused at 1-atm in air and is assumed to have a CO_2 content of zero (the extremely low solubility of CO_2 in basalts and more silica-rich compositions at $pCO_2 = 1$ bar, and the very low mole fraction of CO_2 in air support this assumption e.g., Blank 1993, Stolper and Holloway 1988). The CO_2 content of the spurrite was calculated from stoichiometry, i.e., the mass fraction of CO_2 was adjusted until the cation sum of C and B (on the basis of eleven oxygens) was equal to 1 (the boron content was determined by SIMS using the Cameca IMS 7f-GEO at Caltech; see Krzhizhanovskaya *et al.* 2023 for a discussion of B- and S-bearing spurrite). The calculated CO_2 content (9.36% *m/m*), plus the B_2O_3 content determined by SIMS, plus the remaining oxide concentrations determined by EPMA resulted in an oxide sum of 100.06% *m/m*. We used this stoichiometric approach because the abundant small inclusions on the surface of the polished spurrite sample precluded determining its C content by NRA.

Figure S8 compares the measured CO_2 contents of the secondary reference materials by EPMA with their accepted values and shows that the measurement results are systematically low and offset from the solid 1:1 line. The dashed line, an unweighted least-squares fit to the seven secondary reference materials, has an R^2 value of 0.998. The fact that the best-fit line does not pass through the origin most likely reflects an over-correction of the oxygen interference with the carbon peak. We assumed that the carbon measurement results for the ND-series glasses by

Table 3.
Measured major and volatile composition by electron microprobe (in % *m/m* unless otherwise indicated) of experimental glasses and other glasses analysed during the same measurement sessions

	EPMA (AMNH)													
Experiment #	***n***	**SiO_2**	**TiO_2**	**Al_2O_3**	**FeO_{tot}**	**MnO**	**MgO**	**CaO**	**Na_2O**	**K_2O**	**P_2O_5**	**S (µg g^{-1})**	**Cl (µg g^{-1})**	**Total**
ND 70_ Degassed	5	49.68	0.80	16.12	8.27	0.14	8.71	13.01	2.22	0.16	0.09	15	19	99.19
ND70-2-01	10	47.81	0.76	15.58	8.00	0.15	8.51	12.66	2.17	0.17	0.08	621	753	96.02
ND70-3-01	10	47.18	0.77	15.21	8.04	0.15	8.61	12.76	2.09	0.16	0.08	814	1176	95.23
ND70-4-01	10	47.37	0.75	15.13	7.60	0.16	8.23	12.30	2.19	0.16	0.07	1831	2670	94.39
ND70-4-02	10	44.27	0.73	14.54	7.59	0.14	8.23	12.60	2.21	0.16	0.09	1796	2269	90.97
ND70-5-02	10	46.12	0.65	13.21	6.83	0.12	7.89	13.15	2.34	0.15	0.07	5045	7081	91.75
ND70-6-02	12	44.01	0.64	12.62	6.19	0.11	8.22	13.16	2.12	0.18	0.08	8786	12449	89.46
Other glasses analysed														
ND-70 (Natural)	3	49.92	0.81	16.11	8.17	0.15	8.27	12.95	2.10	0.16	0.09	871	199	98.84
VILLA_P2	12	50.60	1.29	15.42	9.15	0.16	5.41	8.55	3.10	0.75	0.28	3529	120	95.08
INSOL_MX1_BA4	1	52.36	1.62	12.87	8.12	0.11	9.55	10.53	2.66	1.41	0.23	18	114	99.48

n denotes the number of analyses from which means are reported. Uncertainties (expressed as two standard deviation) are ±0.43 for SiO_2, ±0.18 for Na_2O, ±0.02 for K_2O, ±0.17 for Al_2O_3, ±0.36 for CaO, ±0.24 for FeO, ±0.11 for MgO, ±0.04 for TiO_2, ±0.05 for MnO, ±0.04 for P_2O_5, ±0.01 for S and ±0.03 for Cl.

EPMA were similarly offset from their "true" values, and we used the dashed-best-fit line to adjust their CO_2 contents, i.e., to project them onto the *y*-axis in Figure S8. It is these projected ND-series CO_2 mass fractions that are plotted in Figure 2 and listed in Table 4.

EPMA at AMNH

The S, Cl and major element compositions were measured with a Cameca SX5-Tactis at the American Museum of Natural History on a new set of polished glasses mounted in resin. We used an accelerating voltage of 15 kV, a defocused beam of 10 µm, a beam current of 4 nA for Na (with 10 s count time), 10 nA for Mg, Al, Si, Ca (20 s count time), P, K, Ti, Mn, Fe (30 s count time), and 40 nA for S and Cl (count times of 70 s and 40 s respectively). Sodium was determined first to minimise Na loss during measurement. The instrument was calibrated on natural and synthetic mineral reference materials and glasses: albite (Na), olivine (Mg), potassium-feldspar (Al, Si and K), berlinite (P), anorthite (Ca), rutile (Ti), rhodonite (Mn), fayalite (Fe), barium sulfate (S) and scapolite (Cl). Uncertainties (two standard deviation) are ±0.43 for SiO_2, ±0.18 for Na_2O, ±0.02 for K_2O, ±0.17 for Al_2O_3, ±0.36 for CaO, ±0.24 for FeO, ±0.11 for MgO, ±0.04 for TiO_2, ±0.05 for MnO, ±0.04 for P_2O_5, ±0.01 for S and ±0.03 for Cl.

Results

Here we compare results of the different analytical methods against the mass fractions calculated from the quantities loaded into the experimental capsules. Loaded mass fractions are used as a starting point for comparisons with no assumption that they might represent "correct" values. Results from EPMA are given in Table 3, results from ERDA, NRA, FTIR and EA are given in Table 4 and results from SIMS are given in Table 5. Raw SIMS results are given in Tables S3 to S7. SIMS calibration lines are shown in Figures S2 to S7. FTIR spectra and deconvolutions are shown in Figure S9. Raw FTIR spectra are given in Moussallam (2024a). Raw NRA spectra are given in Moussallam (2024b).

H_2O

Water in the new reference glasses was analysed by ERDA, FTIR and at the ion microprobe facilities at CRPG-CNR (Nancy), WHOI, Caltech and JAMSTEC (Kochi). Figure 1 compares the water contents measured by all of these techniques with the expected (i.e., loaded) values. The agreement is in most cases excellent (better than 8%). Significant deviation from the one-to-one line is found for one Caltech Cs^+ beam SIMS analysis of sample ND70-4-02 although the discrepancy between loaded and measure H_2O content in ND70-4-02 disappears if the measured $^{16}O^1H/^{18}O$ ratio is used instead of the $^{16}O^1H/^{30}Si$ ratio. Significant deviation from the one-to-one lines is also found for the Kochi Cs^+ beam SIMS analyses of sample ND70-5-02 and ND70-6-02. Note that these two samples have mass fractions that require very significant extrapolation of the calibration line (Figure S2). Caltech O^- beam SIMS analyses are not shown as most unknown glasses had values outside the calibration range for that session.

Table 4.
ERDA, NRA, EA and FTIR measurement results (in % *m/m* for H_2O and in µg g^{-1} for all other species) of experimental glasses and other glasses analysed during the same measurement sessions

Experiment #	ERDA (CEA-CNRS-Saclay)			NRA (CEA-CNRS-Saclay)			EA (LDEO)			FTIR (LDEO)					EPMA (Caltech)		
	n	H_2O	±	*n*	CO_2	±	*n*	CO_2	±	*n*	H_2O	±	CO_2	±	*n*	CO_2 (µg g^{-1})	±
ND 70_ Degassed																	
ND70-2-01	2	2.53	0.24	1	1837	35				6	2.12	0.34	1283	120			
ND70-3-01	2	3.13	0.30	1	2689	54				7	3.43	0.97	2226	403	5	2997	365
ND70-4-01	1	4.25	0.40	1	4228	71				8	3.86	0.89	4095	621			
ND70-4-02	2	3.68	0.35	1	4122	65									5	4306	794
ND70-5-02	2	5.34	0.51	1	12682	105	1	12160	891	6	5.15	0.59	11868	1204	5	11125	1876
ND70-5-03	1	3.68	0.35														
ND70-6-02	2	6.26	0.59	1	16847	120	1	14940	1095	3	5.85	0.96	15754	1835	5	13397	313
Other glasses analysed																	
ND-70 (Natural)										3	0.66	0.15	59	23			
Suprasil	2	0.02	0.00														
BF73	2	0.73	0.07	1	2832	56				3	0.82	0.06	3042	84	5	6579	3594
BF76										3	0.75	0.06	2319	68	5	3560	266
BF77										3	0.86	0.08	891	47	5	2506	145
M15																	
M19															5	5198	1720
M20	1	5.82	0.55	1	2417	51									5	3056	1160
M34																	
M35	1	4.31	0.41	1	1436	40				3	4.1	0.45	1000	75	5	3119	3414
M40																	
M43										3	2.52	0.25	2857	154	5	3300	536
M48																	
KL2																	
KE12																	
40428																	
47963																	
N72																	
ALV519-4-1																	
ALV1846-12																	
80-1-3																	
ALV1846-9										3	1.43	0.12	18	8			
NS-1										3	0.35	0.03	3546	129	5	4708	1060
Villa_P2										6	3.92	0.7	835	74			
INSOL_MX1_BA4										3	0.15	0.01	8207	377			
VG2																	

All uncertainties are given as one standard deviation on repeat analyses or as one standard deviation from analytical error (whichever is the highest), *n* denotes the number of analyses from which means are reported.

Carbon dioxide

CO_2 in the new reference glasses was measured by NRA, EA, FTIR, EPMA and SIMS (the latter at the ion microprobe facilities at CRPG-CNRS, Nancy, WHOI, Caltech and JAMSTEC, Kochi). Figure 2 compares the CO_2 contents measured by all these techniques with the expected (i.e., loaded) values. Sample ND70_Degassed was measured by SIMS at CRPG-CNRS (Nancy) and JAMSTEC (Kochi). We found that the sample provides a good "blank" for CO_2 with $^{12}C/^{30}Si$ signals comparable to those obtained on pure quartz and San Carlos olivine (Table S8). Figure 2 shows that samples ND70-2-01, ND70-3-01, ND70-4-01, ND70-4-02 and ND70-5-03 have measured CO_2 contents significantly higher than expected based on the loaded amounts of CO_2 (although not all five samples were analysed using all of the techniques or ion probes). For sample ND70-5-02, measured CO_2 contents from NRA and EA analyses were significantly higher than the loaded (i.e., expected) CO_2 concentration. In contrast, EPMA, O^- beam SIMS analyses from Caltech and WHOI and Cs^+ beam SIMS analyses from JAMSTEC (Kochi) were close to the expected concentration, while Cs^+ beam SIMS analyses at CRPG-CNRS (Nancy), WHOI and Caltech yielded significantly lower concentrations. The measured CO_2 content of sample ND70-6-02 by NRA is higher than the

Table 5.
SIMS measurement results (in % *m/m* for H_2O and in µg g^{-1} for all other species) of experimental glasses and other glasses analysed during the same measurement sessions

Experiment #	SIMS (CRPG, Nancy, Cs^+ beam)										
	n	H_2O	±	CO_2	±	S	±	Cl	±	F	±
ND 70_ Degassed	2	0.03	0.00	66	6	17	1	4	0	13	1
ND70-2-01	3	2.21	0.06	1141	101	649	42	876	110	572	40
ND70-3-01	2	2.70	0.07	1397	124	862	56	983	124	745	52
ND70-4-01	2	3.79	0.10	2519	224	***2207***	***142***	2401	302	1896	133
ND70-5-02	2	4.57	0.12	***6566***	***583***	***6211***	***400***	***6777***	***852***	***5538***	***388***
ND70-5-03	2	3.37	0.09	1098	98	175	11	326	41	228	16
ND70-6-02	2	6.37	0.17	***6482***	***576***	***11214***	***722***	***12405***	***1559***	***9725***	***681***
Other glasses analysed											
ND-70 (Natural)	1	1.04	0.03	195	17	916	59	194	24	98	7
M34	3	5.59	0.15	458	41	11	1	36	4	79	6
M35	10	4.14	0.11	1100	98	11	1	33	4	75	5
M40	10	3.31	0.09	2118	188	12	1	33	4	73	5
M43	1	2.70	0.07	3071	273	5	0	29	4	68	5
M48	10	0.82	0.02	477	42	3	0	28	4	64	4
KL2	10	0.01	0.00	157	14	6	0	14	2	58	4
KE12	10	0.16	0.00	116	10	264	17	3419	430	4251	298
40428	9	0.88	0.02	256	23	889	57	349	44	413	29
47963	10	1.23	0.03	229	20	646	42	902	113	638	45
N72	5	0.02	0.00	186	17	4	0	28	4	77	5
VG2	10	0.34	0.01	396	35	1450	93	233	29	160	11

Experiment #	SIMS (WHOI, Cs^+ beam)										
	n	H_2O	±	CO_2	±	S	±	Cl	±	F	±
ND70-2-01	3	2.31	0.10	1204	92	476	57	518	14	550	47
ND70-3-01	2	2.59	0.12	2106	160	582	70	708	20	683	58
ND70-4-01	3	4.16	0.19	3037	231	1553	187	2125	59	1808	155
ND70-4-02	3	3.69	0.17	3026	231	1505	181	1811	50	1665	142
ND70-5-02	3	5.31	0.24	8770	668	***4714***	***567***	***6357***	***177***	***5694***	***487***
ND70-5-03	3	3.85	0.17	1412	108	128	15	300	8	217	19
ND70-6-02	3	7.11	0.32	8216	626	***8525***	***1026***	***11713***	***326***	***10177***	***870***
Other glasses analysed											
ND-70 (Natural)	3	1.02	0.05	120	9	625	75	160	4	86	7
Suprasil	3	0.01	0.00	25	2	0	0	1912	53	3	0
BF73	2	0.87	0.04	2502	191	0	0	36	1	36	3
BF76	2	0.82	0.04	2134	163	0	0	34	1	27	2
BF77	3	0.82	0.04	791	60	0	0	34	1	27	2
M15	3	1.64	0.07	152	12	1	0	21	1	53	5
M19	3	3.06	0.14	2608	199	3	0	21	1	54	5
M20	3	5.76	0.26	1689	129	8	1	25	1	62	5
M34	3	5.52	0.25	332	25	6	1	24	1	60	5
M35	3	4.41	0.20	896	68	5	1	24	1	60	5
M43	3	2.76	0.13	2720	207	2	0	23	1	55	5
M48	3	0.76	0.03	298	23	0	0	19	1	50	4
KE12	3	0.20	0.01	5	0	204	25	3287	92	4220	361
ALV519-4-1	5	0.19	0.01	205	16	614	74	39	1	62	5
80-1-3	3	0.64	0.03	532	41	596	72	47	1	161	14
1846-9	4	1.78	0.08	9	1	236	28	206	6	269	23
NS-1	3	0.42	0.02	4295	327	31	4	24	1	60	5
Villa_P2	3	4.67	0.21	946	72	3638	438	106	3	144	12
INSOL_MX1_BA4	3	0.22	0.01	8314	634	8	1	81	2	271	23
run101@2.asc	3	1.93	0.09	55	4	285	34	570	16	268	23
run10@2.asc	3	4.35	0.20	23	2	20	2	401	11	4	0
ALV_1833-1	3	2.28	0.10	15	1	497	60	553	15	254	22
WOK28-3	3	0.52	0.02	292	22	650	78	45	1	95	8

Experiment #	SIMS (Caltech, Cs^+ beam)										
	n	H_2O	±	CO_2	±	S	±	Cl	±	F	±
ND70-2-01	2	2.49	0.09	1183	117	513	84	***859***	***156***	***1247***	***99***
ND70-3-01	8	3.18	0.12	1851	184	745	122	***1527***	***277***	***1828***	***145***
ND70-4-02	3	2.99	0.11	2039	202	1219	199	***2061***	***374***	***2658***	***210***

Table 5 (continued).
SIMS measurement results (in % *m/m* for H_2O and in µg g^{-1} for all other species) of experimental glasses and other glasses analysed during the same measurement sessions

	SIMS (Caltech, Cs^+ beam)										
Experiment #	*n*	H_2O	±	CO_2	±	S	±	Cl	±	F	±
ND70-5-02	2	4.94	0.18	8151	808	***4687***	***766***	***8955***	***1626***	***12118***	***959***
ND70-6-02	2	6.95	0.26	7234	718	***7687***	***1257***	***15406***	***2798***	***20358***	***1611***
Other glasses analysed											
ND-70 (Natural)	2	1.09	0.04	135	13	657	107	257	47	193	15
Suprasil	2	0.00	0.00	2	0	0	0	***2456***	***446***	0	0
BF73	2	0.79	0.03	2435	242	0	0	53	10	73	6
BF76	2	0.85	0.03	2534	251	0	0	54	10	61	5
BF77	2	0.83	0.03	853	85	0	0	51	9	57	5
M15	2	1.68	0.06	138	14	1	0	32	6	115	9
M19	2	3.41	0.13	2520	250	3	1	35	6	122	10
M20	2	5.36	0.20	1609	160	8	1	39	7	132	10
M34	1	5.40	0.20	265	26	6	1	34	6	124	10
M35	2	4.15	0.15	869	86	5	1	34	6	126	10
M43	1	2.80	0.10	2834	281	2	0	35	6	121	10
M48	1	0.84	0.03	221	22	0	0	31	6	113	9
ALV519-4-1	2	0.16	0.01	189	19	541	88	46	8	111	9
1846-12	2	1.38	0.05	126	12	617	101	347	63	282	22
80-1-3	2	0.55	0.02	365	36	566	93	60	11	317	25
1846-9	2	1.71	0.06	7	1	223	36	275	50	574	45
NS-1	3	0.42	0.02	4931	489	32	5	36	6	135	11
Villa_P2	2	4.52	0.17	909	90	3698	604	151	27	303	24
INSOL_MX1_BA4	2	0.18	0.01	7737	767	6	1	95	17	492	39
run101@2.asc	2	1.74	0.06	49	5	252	41	781	142	548	43
run10@2.asc	2	3.78	0.14	14	1	16	3	482	88	2	0
	SIMS (SIMS (JAMSTEC, Kochi) Cs^+ primary beam)										
Experiment #	*n*	H_2O	±	CO_2	±	S	±	Cl	±	F	±
Experiment #	*n*	H_2O	±	CO_2	±	S	±	Cl	±	F	±
ND 70_ Degassed	2	0.03	0.00	8	0	39	1	12	1	16	1
ND70-2-01	3	2.55	0.09	1339	61	709	24	495	44	722	39
ND70-3-01	3	3.32	0.11	2121	96	1017	34	1068	96	982	53
ND70-4-01	3	4.62	0.16	3320	151	***2365***	***80***	2276	204	2355	126
ND70-4-02	3	3.96	0.14	3421	155	***2238***	***76***	2101	188	2109	113
ND70-5-02	3	***6.00***	***0.21***	***10034***	***455***	***6982***	***236***	***7095***	***636***	***7543***	***404***
ND70-6-02	3	***7.81***	***0.27***	***11934***	***542***	***12567***	***426***	***12606***	***1130***	***13703***	***735***
Other glasses (and minerals) analysed											
ND-70 (Natural)	2	1.06	0.04	200	9	883	30	176	16	105	6
Vol-std-G_EPR-G3	5	0.24	0.01	355	16	1236	42	118	11	117	6
Vol-std-G_SC-ol	1	0.00	0.00	9	0	0	0	0	0	1	0
Vol-std-G_ELA-qz	4	0.01	0.00	12	1	0	0	0	0	1	0
Vol-std-G_IND-G1	1	0.51	0.02	206	9	1043	35	78	7	172	9
Vol-std-G_Vol-3A	1	3.46	0.12	4786	217	1046	35	2547	228	2996	161
Vol-std-G_Vol-1B	1	0.94	0.03	4546	206	673	23	743	67	847	45
Vol-std-G_Vol-05A	1	0.57	0.02	3384	154	521	18	272	24	418	22
Vol-std-G_Vol-005B	1	0.09	0.00	503	23	44	1	32	3	46	2
Vol-std-G_MRN-G1	1	2.12	0.07	6	0	72	2	2854	256	650	35
Vol-std-G_MA42	1	4.74	0.16	1492	68	29	1	111	10	72	4
Vol-std-G_FJ-G2	1	0.24	0.01	429	19	1328	45	90	8	117	6
Vol-std-G_IND-G2	1	0.54	0.02	482	22	1042	35	80	7	209	11
Vol-std-G_vol-0B	1	0.02	0.00	8	0	1	0	1	0	5	0
	SIMS (WHOI, O^- beam)										
Experiment #	*n*	H_2O	±	CO_2	±	S	±	Cl	±	F	±
ND70-2-01	3	2.70	0.11	1315	148						
ND70-3-01	5	3.31	0.14	1721	193						
ND70-4-01	5	4.21	0.18	3595	404						
ND70-4-02	3	3.49	0.15	3219	362						
ND70-5-02	3	4.62	0.19	***10855***	***1220***						
ND70-5-03	3	3.79	0.16	1655	186						
ND70-6-02	3	5.96	0.25	***11981***	***1346***						

Table 5 (continued).
SIMS measurement results (in % *m/m* for H_2O and in µg g^{-1} for all other species) of experimental glasses and other glasses analysed during the same measurement sessions

	SIMS (WHOI, O⁻ beam)										
Experiment #	***n***	**H_2O**	**±**	**CO_2**	**±**	**S**	**±**	**Cl**	**±**	**F**	**±**
Other glasses analysed											
ND-70 (Natural)	3	1.12	0.05	163	18						
Suprasil	3	0.01	0.00	30	3						
M20	3	5.49	0.23	1851	208						
M35	3	4.10	0.17	927	104						
ALV519-4-1	3	0.20	0.01	215	24						
NS-1	3	0.48	0.02	4254	478						
Villa_P2	3	4.26	0.18	1040	117						
INSOL_MX1_BA4	3	0.24	0.01	7718	867						
	SIMS (Caltech, O⁻ beam)										
Experiment #	***n***	**H_2O**	**±**	**CO_2**	**±**						
ND70-2-01	2	2.42	0.15	1343	184						
ND70-3-01	8	***3.05***	***0.19***	1979	271						
ND70-4-02	3	***3.40***	***0.21***	3309	454						
ND70-5-02	2	***4.31***	***0.26***	***9928***	***1361***						
ND70-6-02	2	***5.26***	***0.32***	***11615***	***1593***						
Other glasses analysed											
ND-70 (Natural)											
Suprasil	1	0.00	0.00	0	0						
M43	1	2.58	0.16	2806	385						
80-1-3	2	0.68	0.04	626	86						
NS-1	3	0.45	0.03	4223	579						
INSOL_MX1_BA4	2	0.23	0.01	7729	1060						

Uncertainties are calculated using two standard error (i.e., 95% confidence interval) on calibration lines for each session, *n* denotes the number of analyses from which means are reported. Values in bold italics were determined outside calibration range.

amount loaded, close to the expected amount when using EA and FTIR, but significantly lower than the amount loaded when considering EPMA and all SIMS analyses (regardless of primary species). The mismatch between loaded and measured CO_2 contents in most experiments may reflect C contamination either during sample preparation or during the experiment. Carbon diffusion through platinum capsules has been documented by Brooker *et al.* (1998) at temperatures around 1650 °C, significantly higher than the temperatures used here and no "blackening" of our glasses was observed.

Sulfur

Sulfur in the new reference glasses was measured by EPMA at AMNH and at the ion microprobe facilities at CRPG-CNRS (Nancy), WHOI, Caltech and JAMSTEC (Kochi). Figure 3 compares the loaded S contents with the mass fractions measured by EPMA and the four ion probes. The agreement is excellent for samples ND70_Degassed, ND70-2-01, ND70-3-01, ND70-5-03 and, except for the Kochi analyses, ND70-5-02. Samples ND70-4-01 and ND70-4-02 show somewhat lower than expected values in the Caltech and WHOI SIMS analyses. Compared with the loaded concentration, the measured S content in sample ND70-6-02 was significantly lower in the EPMA and Caltech and WHOI SIMS analyses and higher in the Nancy and Kochi SIMS analyses. Note that the SIMS S measurements for both ND70-5-02 and ND70-6-02 are based on very significant extrapolation from calibration ranges (Figure S4).

Chlorine

Chlorine in the new reference glasses was measured by EPMA at AMNH and at the ion microprobe facilities at CRPG-CNRS (Nancy), WHOI, Caltech and JAMSTEC (Kochi) (the Caltech analyses are not shown as most of the unknown glasses had values outside the calibration range for that session). Figure 4 compares the Cl contents measured by these techniques with the expected (i.e., loaded) values. Samples ND70_Degassed, ND70-2-01, ND70-3-01, ND70-4-01, ND70-4-02 and ND70-5-03 all show good to excellent agreements. The measured Cl contents in

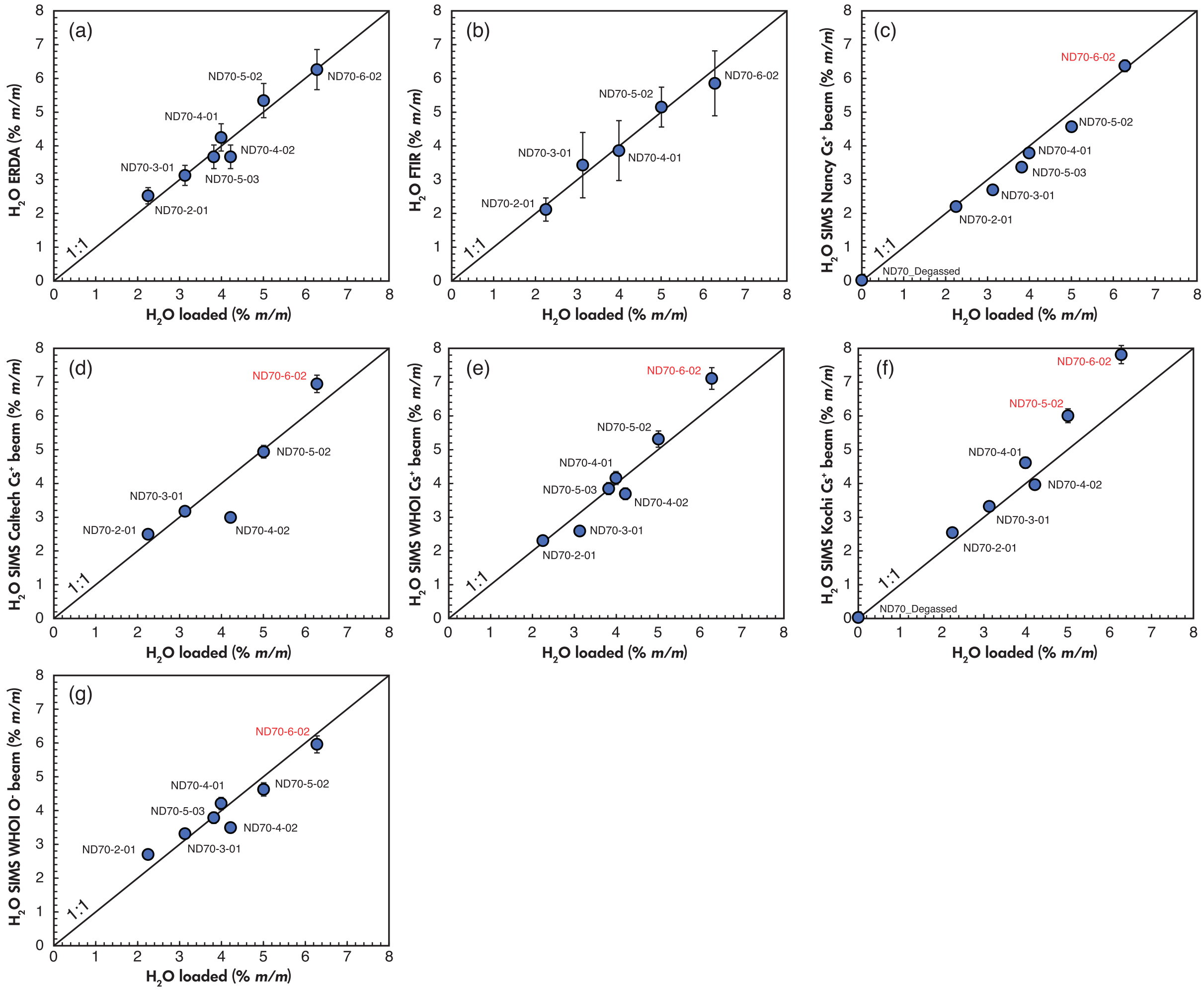

Figure 1. Comparison between the expected (i.e., loaded) and measured water content in the new reference materials. Samples labelled in red were measured outside their respective calibration ranges (Figure S2).

samples ND70-5-02 and ND70-6-02 are significantly higher than loaded amounts in all three sets of SIMS analyses and in the electron probe analyses. Note that the SIMS Cl measurements for both ND70-5-02 and ND70-6-02 are based on very significant extrapolation from calibration ranges (Figure S5).

Fluorine

Fluorine in the new reference glasses was measured at the ion microprobe facilities at CRPG-CNRS (Nancy), WHOI, JAMSTEC (Kochi) and Caltech, but the Caltech analyses are not shown as most of the unknown glasses had F mass fractions outside the calibration range for that session. Figure 5 compares the F contents measured by the Nancy, WHOI and Kochi ion probes with the expected (i.e., loaded) values. Samples ND70_Degassed, ND70-2-01, ND70-3-01, ND70-4-01, ND70-4-02 and ND70-5-03 all show good to excellent agreements between the measured and expected mass fractions. For samples ND70-5-02 and ND70-6-02 where measurements are based on very significant extrapolation from calibration ranges (Figure S6) the agreement is excellent for the Nancy and WHOI SIMS analyses but the Kochi analyses for these glasses are significantly higher.

Reference material homogeneity

Based on volatile solubility experiments described in the literature (e.g., Stolper and Holloway 1988, Blank and Brooker 1994, Lesne *et al.* 2011, Iacono-Marziano *et al.* 2012, Moussallam, *et al.* 2015, Allison *et al.* 2019)

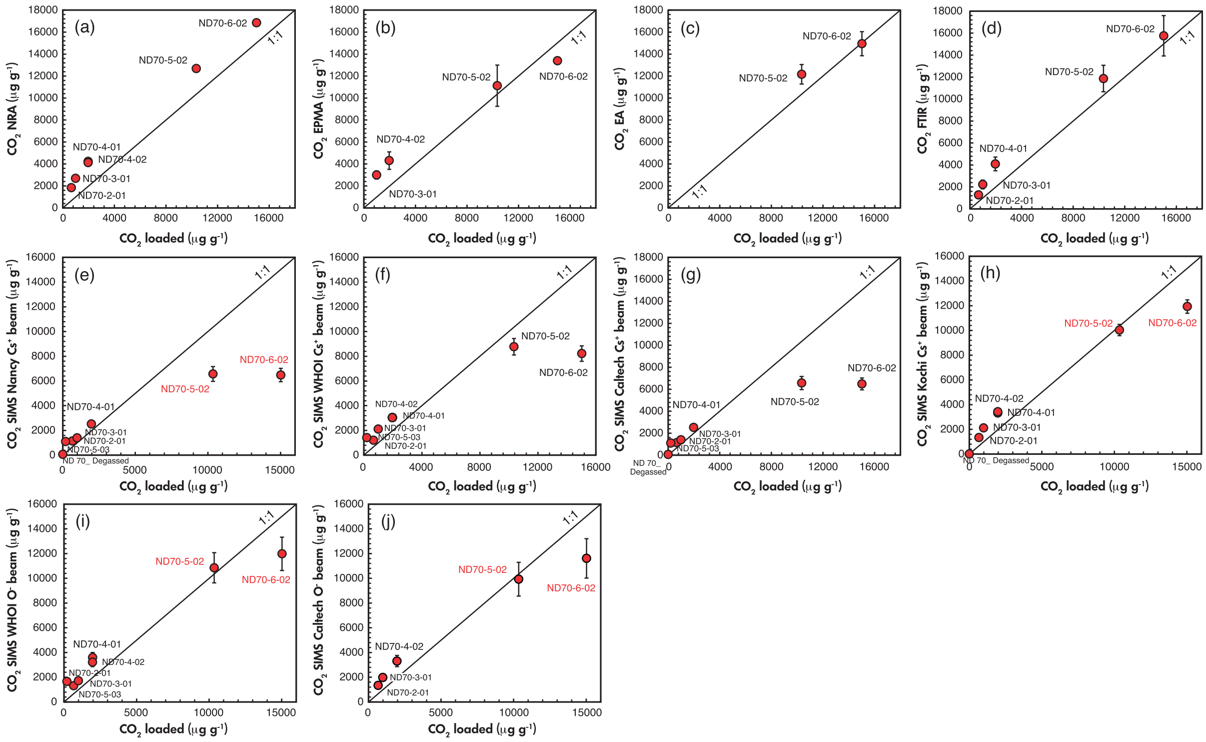

Figure 2. Comparison between the expected (i.e., loaded) and measured CO_2 content in the new reference materials. Samples labelled in red were measured outside their respective calibration ranges (Figures S3 and S7).

our experimental durations and temperatures should have been sufficient to achieve homogeneity in term of both major and volatile element distributions in the experimental glasses (recall that the starting material was a twice-fused glass). Evidence of homogeneity is further provided by the good inter-instrument comparison (see following section). Except for the WHOI and Caltech SIMS analyses, which were performed on the same mount (i.e., the same pieces of glass), all other techniques were performed on distinct sets of glasses.

Discussion

Inter-instrument comparison

Figure 6 compares the mean absolute deviation (i.e., $\frac{\sum normalized(|\Delta|)}{n}$, in %) between all the techniques used to measure H_2O, CO_2, S, Cl and F contents in the ND70 suite, and Figure 7 graphically compares all the measurements. For H_2O, results from ERDA, FTIR and five SIMS sessions all agree with average mean absolute deviations around 10% between methods. The JAMSTEC-Kochi SIMS results show larger deviations (15% on average) but this is entirely due to samples ND70-5-02 and ND70-6-02 being outside the calibration range for that SIMS session. For CO_2, NRA, EA, FTIR and EPMA analyses agree on average within ±9%. Cs^+ primary beam SIMS analyses at Caltech, WHOI and Nancy agree reasonably well with each other (on average within ±18%) but agree poorly with the other techniques due to the low values measured in samples ND70-5-02 and ND70-6-02, which were outside the calibration range for the Nancy SIMS session and dominate the mean absolute deviation calculation (more on this in the following section). Cs^+ primary beam SIMS analyses at Kochi however agree with O^- primary beam SIMS analyses at Caltech and WHOI (on average within ±5%), and agrees poorly with the other Cs^+ primary beam SIMS analyses (on average within ±33%). O^- primary beam SIMS analyses at Caltech and WHOI agree with each other within ±6% and are in reasonable agreement with the results from NRA, EA and FTIR, on average within ±19%, but differ from the EPMA mass fractions by, on average, ±27%. Note that only two samples were analysed by EA, partially explaining why this technique shows the lowest average mean absolute deviation.

For S, the means of the electron probe measurements and the four sets of Cs^+ primary beam SIMS measurements (Caltech, WHOI, Kochi and Nancy) all agree within

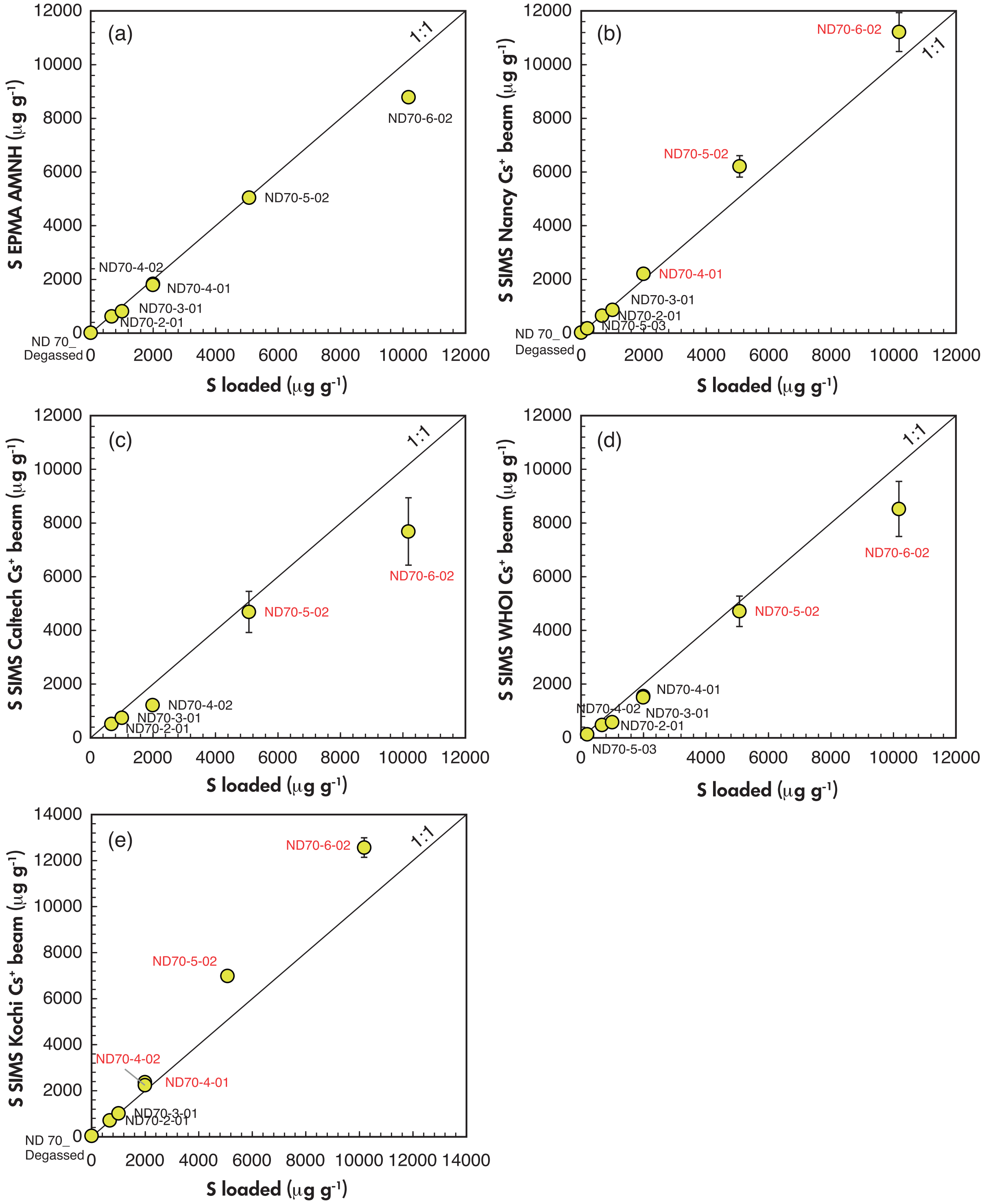

Figure 3. Comparison between the expected (i.e., loaded) and measured S content in the new reference materials. Samples labelled in red were measured outside their respective calibration ranges (Figure S4).

approximately ±30% with much of this uncertainty being dominated by the large differences between the Kochi and WHOI measurements. For Cl, the means of the electron probe measurements and the three sets of Cs^+ primary beam SIMS measurements (WHOI, Nancy and Kochi) all agree, on average, within ±17%; the agreement is similar when the means are compared with the loaded amounts of Cl despite samples ND70-5-02 and ND70-6-02 being outside the calibration range for the SIMS measurements. The EPMA, Nancy and Kochi SIMS measurements all agree

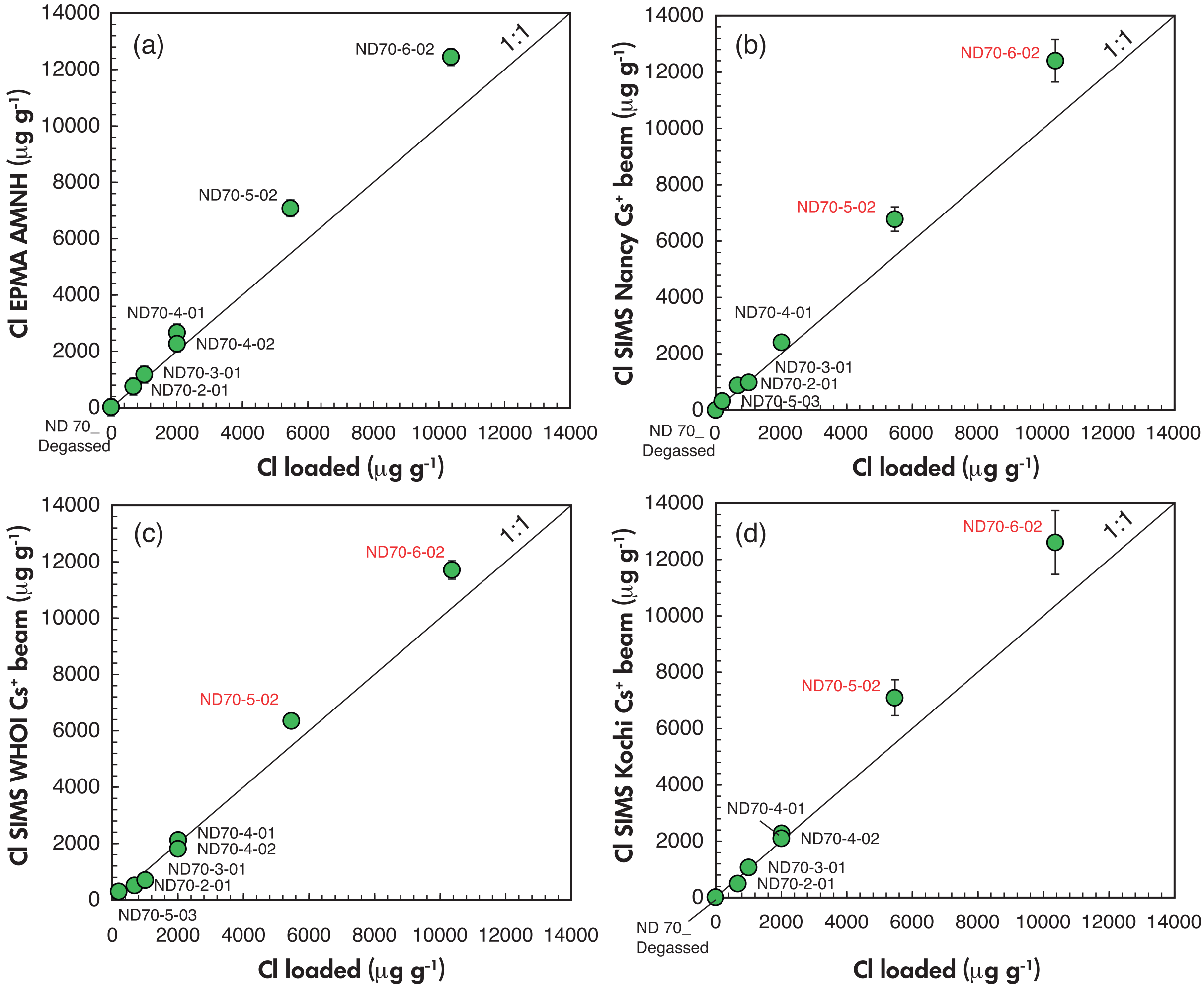

Figure 4. Comparison between the expected (i.e., loaded) and measured Cl content in the new reference materials. Samples labelled in red were measured outside their respective calibration ranges (Figure S5).

on average within ±11%. In contrast, the agreement between the WHOI measurements and the other techniques is poorer (due to strong deviations on samples ND70-5-02 and ND70-6-02). For F, all three SIMS sessions (WHOI, Nancy, Kochi) agree with the loaded values, within ~ 14%, on average despite samples ND70-5-02 and ND70-6-02 being outside the calibration range for all SIMS sessions. The WHOI and Nancy SIMS sessions agree best, on average, within ±10%, while the Kochi session agreement is poorer (due to strong deviations on samples ND70-5-02 and ND70-6-02).

Effect of water on SIMS CO_2 measurements

All four Cs^+ primary beam SIMS sessions (Kochi, Caltech, WHOI and Nancy), yielded CO_2 contents for ND70-6-02, that were low relative to the loaded abundance of CO_2. The loaded CO_2 abundance in sample ND70-6-02 was 1.5% *m/m* (verified by FTIR, EA and NRA), yet the Cs^+ primary beam SIMS analyses at all four ion probes measured $^{12}C/^{30}Si$ ratios much lower than expected for such a mass fraction (see Figure S3). In three out of four cases, the measured $^{12}C/^{30}Si$ ratios were even lower than those measured in sample ND70-5-02, which contained 1% *m/m* CO_2. We attribute this anomaly to the high water mass fraction in the ND70-6-02 glass (> 6% *m/m*), limiting the ionisation efficiency of ^{12}C, a phenomenon previously reported in an AGU abstract by Hervig *et al.* (2009) and similar to the decreasing yield of H^- ions observed with increasing water mass fraction (e.g., Hauri *et al.* 2002, Befus *et al.* 2020) although in this case the species are different.

Figure 8 shows the ionisation efficiency ratios, (($^{12}C/^{30}Si$) × SiO_2)/CO_2 and ($^{12}C/^{18}O$)/CO_2, as a function of the

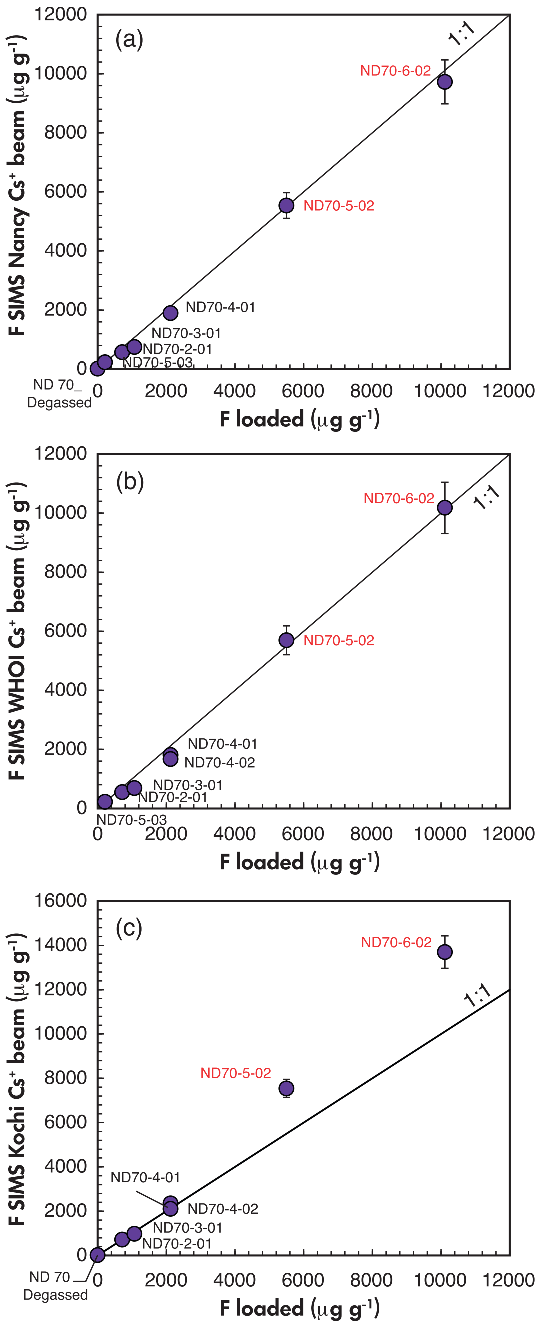

Figure 5. Comparison between the expected (i.e., loaded) and measured F content in the new reference materials. Samples labelled in red were measured outside their respective calibration ranges (Figure S6).

water content in all the glasses analysed during all SIMS sessions (note, we have not plotted glasses with CO_2 content near 0). If water had no effect on the ^{12}C ion probe signal, both ratios should remain constant as a function of water content. What was observed, however, was that these ratios varied greatly. At low water contents (< 2% *m/m*), the ratios are quite variable; in the Caltech and WHOI SIMS sessions, there is a hint of a possible positive correlation between C ionisation efficiency and the glass water content, peaking at ~ 1.5% *m/m* H_2O. At higher water contents (> 2% *m/m*), the C ionisation efficiency seems to become more stable, at least in the explored range (2.5 to 6% *m/m* H_2O), although there is still a hint of an inverse correlation between water content and C ionisation efficiency (Figure 8a, b). The fact that the C ionisation efficiency is so variable between SIMS sessions suggests that the magnitude of the effect may be related to beam conditions.

Although Hervig *et al.* (2009) reported that using an O^- primary beam significantly mitigates the influence of H_2O on the carbon ion yield, we found that O^- primary beam analyses also suffered from the same effect (Figure 8c, d; note that the magnitude of the effect, although based on a smaller number of analyses, may potentially be less), The consequences of this C ionisation efficiency reduction for SIMS carbon analyses are potentially dire. For example, if one were to determine carbon in a natural basaltic glass containing 4% *m/m* water using a Cs^+ primary beam and glass reference materials with less than 2% *m/m* water, the unknown CO_2 mass fractions could be underestimated by two to three-fold. The corollary is also true, using reference materials with high water contents to measure CO_2 mass fractions in samples with low water contents will result in large overestimations. It is likely that these effects permeate the literature of published glass and melt inclusion CO_2 concentration data. Thus, to accurately measure CO_2 by SIMS, one needs to select reference materials with water mass fractions matching those of the unknown sample or to characterise the signal dependency on water content as in Figure 8.

Recommended values for ND70 glasses

The compositions of the new reference materials we consider to be the most accurate, and which we encourage

Figure 6. Matrices showing the mean absolute deviation (in %) between all techniques used to measure H_2O, CO_2, S, Cl and F contents in the new reference materials. Background boxes colours are scaled with the mean absolute deviation from green to red. For each box, the mean absolute deviation is calculated by summing all absolute differences between the volatile contents determined by the row and column techniques normalised by the row technique and dividing by the number of analyses.

H_2O	ERDA	FTIR	SIMS Cs^+ Caltech	SIMS Cs^+ WHOI	SIMS O^- WHOI	SIMS Cs^+ Nancy	SIMS Cs^+ Kochi	Mean*
Loaded	6	6	11	8	9	7	14	9
ERDA		9	8	7	6	10	10	8
FTIR			12	13	10	10	19	11
SIMS Cs^+ Caltech				12	10	11	15	11
SIMS Cs^+ WHOI					12	9	13	11
SIMS O^- WHOI						11	15	10
SIMS Cs^+ Nancy							20	11
SIMS Cs^+ Kochi								15

CO_2	NRA	EA	FTIR	SIMS Cs^+ Caltech	SIMS O^- Caltech	SIMS Cs^+ WHOI	SIMS O^- WHOI	SIMS Cs^+ Nancy	SIMS Cs^+ Kochi	EPMA	Mean*
Loaded	101	9	69	48	59	140	155	115	64	85	85
NRA		8	13	42	25	32	24	47	23	12	33
EA			4	42	20	36	15	51	19	9	21
FTIR				28	15	22	14	38	14	19	23
SIMS Cs^+ Caltech					33	17	35	14	37	74	37
SIMS O^- Caltech						13	6	31	3	27	23
SIMS Cs^+ WHOI							20	21	16	44	36
SIMS O^- WHOI								30	8	31	34
SIMS Cs^+ Nancy									48	97	49
SIMS Cs^+ Kochi										23	25
EPMA											42

S	EPMA AMNH	SIMS Cs^+ Caltech	SIMS Cs^+ WHOI	SIMS Cs^+ Nancy	SIMS Cs^+ Kochi	Mean*
Loaded	10	24	25	12	17	18
EPMA AMNH		16	15	15	29	17
SIMS Cs^+ Caltech			13	30	54	27
SIMS Cs^+ WHOI				38	140	46
SIMS Cs^+ Nancy					12	21
SIMS Cs^+ Kochi						50

Cl	Loaded	EPMA AMNH	SIMS Cs^+ WHOI	SIMS Cs^+ Nancy	SIMS Cs^+ Kochi	Mean*
Loaded		20	21	19	17	19
EPMA AMNH			21	10	11	16
SIMS Cs^+ WHOI				24	16	21
SIMS Cs^+ Nancy					13	16
SIMS Cs^+ Kochi						14

F	Loaded	SIMS Cs^+ WHOI	SIMS Cs^+ Nancy	SIMS Cs^+ Kochi	Mean*
Loaded		15	12	15	14
SIMS Cs^+ WHOI			5	33	18
SIMS Cs^+ Nancy				30	16
SIMS Cs^+ Kochi					26

*Mean of *mean absolute deviation* across methods (in %)

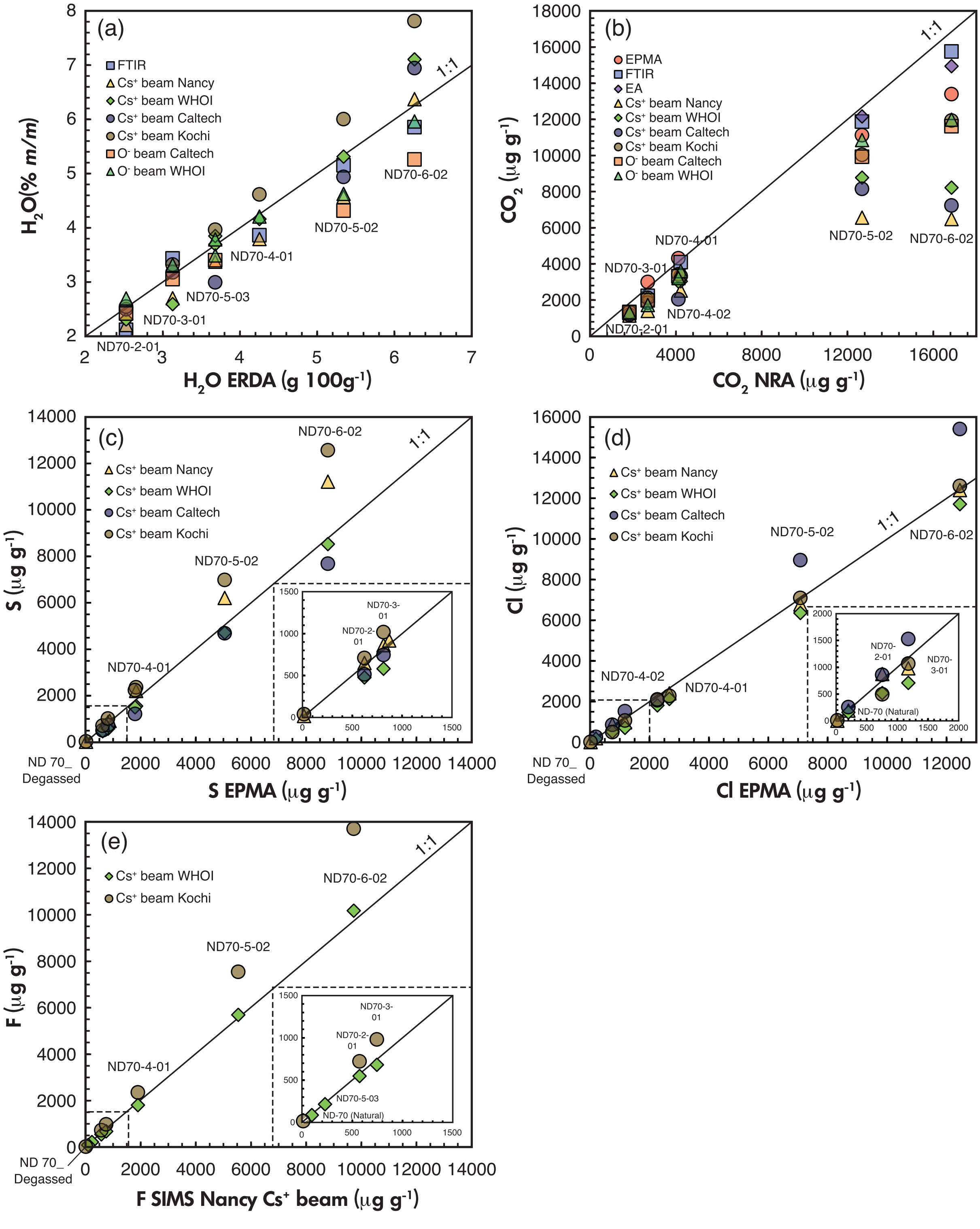

Figure 7. **Comparison of measured H_2O, CO_2, S, Cl and F volatile content in ND70-series glasses by several techniques. With the exception of the last panel, the *x*-axis of each plot is the technique we have highest confidence in. All F determinations (panel E) were acquired using SIMS. The *y*-axes give the value measured by all other techniques.**

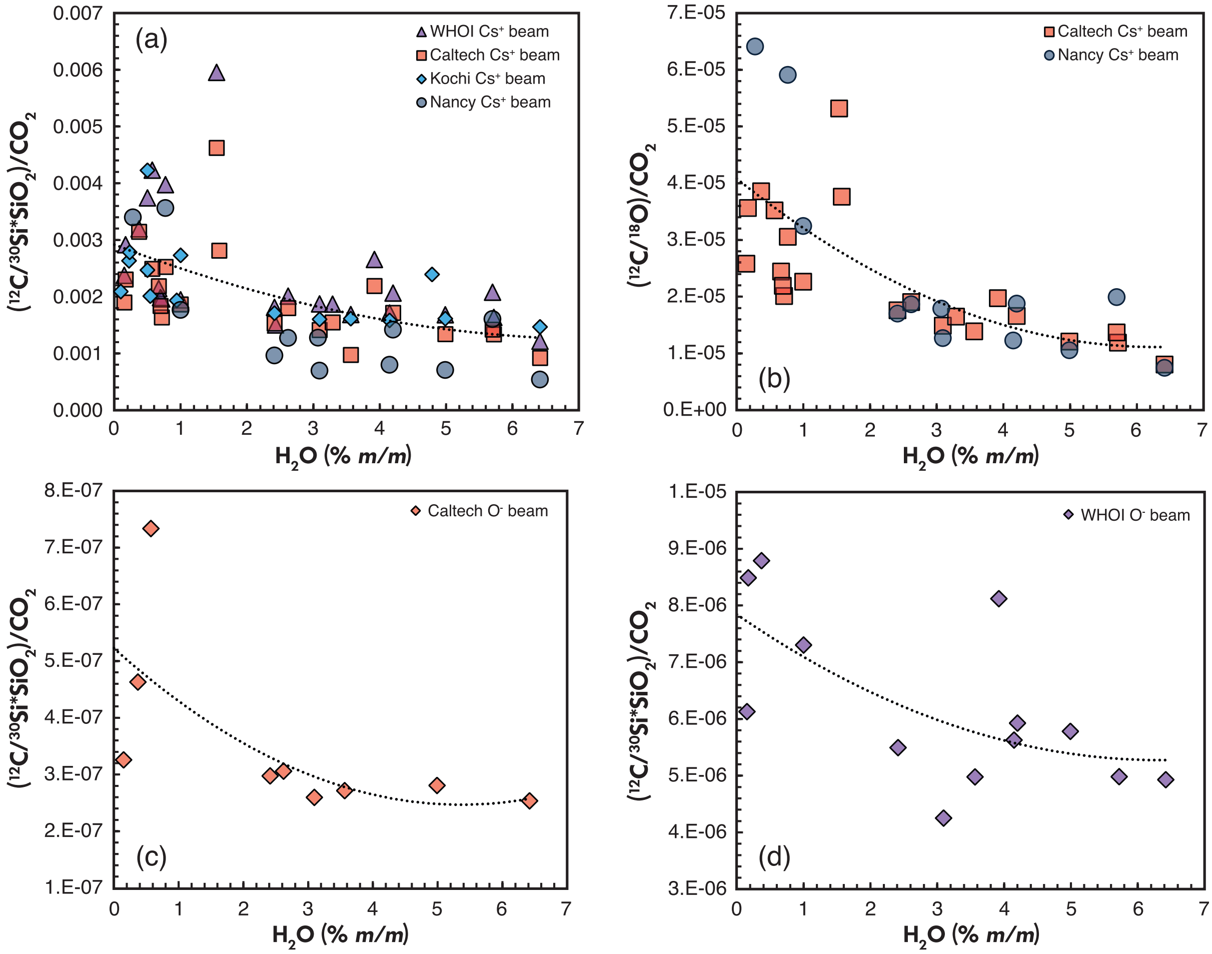

Figure 8. Effect of water on the (($^{12}C/^{30}Si$) × SiO_2)/CO_2 and ($^{12}C/^{18}O$)/CO_2 ratios measured by SIMS (i.e., the calibration line). The results of four SIMS sessions using a Cs^+ primary beam and two SIMS sessions using an O^- primary beam are reported. In all cases the glass water content seems to greatly reduce the ionisation efficiency of ^{12}C. Data used to generate the figure are reported in Table S9. Dotted lines are 2nd-order polynomial best fit to all data.

researchers to use in future studies are reported in Table 6. For H_2O, since all techniques agree within 13% (Figure 6), we used the unweighted arithmetic mean values from ERDA, FTIR, the three Cs^+ primary beam SIMS sessions at Caltech, WHOI and Nancy, the O^- primary beam session at WHOI and the Cs^+ primary beam SIMS session at Kochi (excluding samples ND70-5-02 and ND70-6-02 which were outside calibration range for the Kochi session). We report the uncertainty as the standard deviation from these means. For CO_2, given the strong effect of water on suppressing C ionisation efficiency (see previous section), we used the unweighted arithmetic mean of the NRA, EA and FTIR measurement results and, for the low C (< 5000 µg g^{-1}) samples, we also included the EPMA measurement results. We report the uncertainty as the standard deviation from these means. For ND70_Natural we report the unweighted arithmetic mean of all SIMS and FTIR sessions along with the associated standard deviation. For S, since all techniques agreed reasonably well, we used the unweighted arithmetic mean values from EPMA and the four Cs^+ primary beam SIMS sessions (Caltech, WHOI, Kochi and Nancy) and report the uncertainty as the standard deviation from these means. For Cl, we used the unweighted arithmetic mean values from EPMA and three Cs^+ primary beam SIMS sessions at WHOI, Nancy and Kochi (but excluding samples ND70-5-02 and ND70-6-02 from the WHOI session which deviated significantly from all other estimates) and report the uncertainty as the standard deviation from these means. For F, we used the mean values from three Cs^+ primary beam SIMS sessions at WHOI, Nancy and Kochi (excluding samples ND70-5-02 and ND70-6-02 from the Kochi session which deviated significantly from all other estimates)

Table 6.
Major element and volatile content of the new reference glasses

Sample No.	IGSN	NMNH catalogue number	Major elements (normalised)						
			SiO_2	TiO_2	Al_2O_3	FeO_{tot}	MnO	MgO	CaO
ND 70_ Degassed	10.58052/IEYM10001	118554-1	50.09	0.80	16.25	8.34	0.14	8.78	13.11
ND-70 (Natural)		118554-8	50.56	0.82	16.32	8.27	0.15	8.38	13.12
ND70-2-01	10.58052/IEYM10002	118554-2	49.86	0.79	16.25	8.34	0.16	8.87	13.20
ND70-3-01	10.58052/IEYM10003	118554-3	49.64	0.81	16.00	8.46	0.15	9.06	13.42
ND70-4-01	10.58052/IEYM10004	118554-4	50.43	0.80	16.10	8.09	0.17	8.76	13.09
ND70-4-02	10.58052/IEYM10005	118554-5	48.88	0.80	16.05	8.39	0.16	9.09	13.92
ND70-5-02	10.58052/IEYM10006	118554-6	50.94	0.72	14.59	7.55	0.13	8.72	14.52
ND70-6-02	10.58052/IEYM10007	118554-7	50.39	0.73	14.45	7.09	0.13	9.41	15.06

For H_2O we used the mean values from ERDA, FTIR, the three Cs^+ primary beam SIMS sessions at Caltech, WHOI and Nancy, the O^- primary beam session at WHOI and the Cs^+ primary beam SIMS sessions at Kochi but excluding samples ND70-5-02 and ND70-6-02, outside calibration range in that session. We report the uncertainty as the standard deviation from these means. For CO_2 we used the mean of the NRA, EA and FTIR measurement results and, for the low C (< 5000 µg g^{-1}) samples, we also included the EPMA results. We report the uncertainty as the standard deviation from these means. For ND70_Natural we report the mean of all SIMS and FTIR sessions along with the associated standard deviation. For S, we used the mean values from EPMA and the four Cs^+ primary beam SIMS sessions (Caltech, WHOI, Kochi and Nancy) and report the uncertainty as the standard deviation from these means. For Cl, we used the mean values from EPMA and three Cs^+ primary beam SIMS sessions at WHOI, Nancy and Kochi (but excluding samples ND70-5-02 and ND70-6-02 from the WHOI session which deviated significantly from all other estimates) and report the uncertainty as the standard deviation from these means. For F, we used the mean values from three Cs^+ primary beam SIMS sessions at WHOI, Nancy and Kochi (but excluding samples ND70-5-02 and ND70-6-02 from the Kochi session which deviated significantly from all other estimates) and report the uncertainty as the standard deviation from these means. International Generic Sample Number (IGSN) and catalogue numbers from the Smithsonian National Museum of Natural History (NMNH) Rock and Ore Collections are provided.

and report the uncertainty as the standard deviation from these means.

ND70 glasses, use and availability

The ND70 reference materials are now readily accessible to users at various ion microprobe facilities, including those in France (CNRS-CRGP, Nancy and INSU-CNRS-IMPMC, Paris), the United Kingdom (NERC, Edinburgh), Switzerland (SNF, Lausanne), the United States (WHOI, Arizona State University and Caltech), and Japan (JAMSTEC, Kochi). Furthermore, these resources are available for researchers to borrow from the Smithsonian National Museum of Natural History. Catalogue numbers for these materials are given in Table 6. We encourage researchers to use at least a subset of these glasses (depending on the range of interest) to improve the inter-comparability of future studies presenting microbeam measurements of H_2O, CO_2, S, Cl and F in basaltic glasses. In particular, we expect the high volatile glasses to fill a gap in the reference materials currently available at most ion microprobe facilities.

Conclusions

We present a new set of reference materials designed for *in situ* measurement of volatile elements (H_2O, CO_2, S, Cl, F) in basaltic silicate glass. The starting material was fused in air and 150 to 200 mg splits with variable amounts of volatiles were subsequently run in the piston cylinder. The resulting reference glasses (the ND-70 series) span a wide range of mass fractions from 0 to 6% *m/m* H_2O, 0 to 1.6% *m/m* CO_2, and 0 to 1% *m/m* S, Cl and F. The samples were characterised by elastic recoil detection analysis, nuclear reaction analysis, elemental analyser, Fourier transform infrared spectroscopy, secondary ion mass spectrometry and electron probe microanalyser.

Most analytical techniques provided good agreement with the expected volatile mass fractions in each of the glasses; agreement between techniques and between different ion probes is also generally good. CO_2 measurements are the exception and deviated significantly from expected values across analytical methods; however, inter-method reproducibility was good except for SIMS measurements. We found that this discrepancy in the SIMS results was likely due to the samples' high-water contents, which have a substantial impact on the ionisation efficiency of ^{12}C during SIMS analyses. This underscores the importance of carefully selecting reference materials with water mass fractions matching those of unknown samples or characterising the signal dependency on water content to ensure accurate CO_2 measurements by SIMS.

The reference materials we have presented in this study offer a community resource for the determination of volatile elements in basaltic silicate glass, particularly when using

				Volatiles									
Na_2O	K_2O	P_2O_5	sum	H_2O	±	CO_2 (µg g^{-1})	±	S (µg g^{-1})	±	Cl (µg g^{-1})	±	F (µg g^{-1})	±
2.23	0.16	0.09	100	blank		blank		24	13	11	8	15	2
2.13	0.16	0.09	100	1.00	0.17	145	53	790	138	182	18	96	9
2.26	0.17	0.08	100	2.41	0.21	1560	392	594	97	661	185	615	93
2.20	0.17	0.08	100	3.09	0.32	2637	388	804	160	984	200	803	158
2.33	0.17	0.07	100	4.15	0.30	4161	94	1989	367	2368	231	2020	294
2.43	0.18	0.10	100	3.56	0.36	4214	130	1689	435	2060	232	1887	314
2.58	0.16	0.08	100	4.99	0.34	12237	412	5528	1023	6984	180	5616	110
2.43	0.21	0.09	100	6.42	0.51	15847	957	9756	2047	12293	396	9951	319

SIMS and other microbeam techniques. These materials are available to users at the ion microprobe facilities in France (CNRS-CRGP, Nancy and INSU-CNRS-IMPMC, Paris), the United Kingdom (NERC, Edinburgh), Switzerland (SNF, Lausanne), the United States (WHOI, ASU and Caltech) and Japan (JAMSTEC, Kochi). They are also freely available to researchers on a loan basis from the Smithsonian National Museum of Natural History (Catalogue numbers given in Table 6). We encourage researchers to utilise them to improve the accuracy and inter-laboratory comparability of their measurements.

Acknowledgements

We thank Nordine Bouden and Johan Villeneuve for their invaluable support during the ion probe analyses at CNRS-CRPG, Nancy. We are very grateful to Richard Hervig and an anonymous reviewer for their comments, which greatly improved the manuscript, and to Thomas Meisel for editorial handling. The author contributions, indicated by initials in parentheses, were as follows: Initial study design (WHT, YM, TP), Experiments (WHT, YM, SD), ERDA (HB, HK), NRA (HB, HK), EA (HL), FTIR (SD, HL, SS), SIMS (Nancy) (YM, ERK), SIMS (WHOI) (BM, GG), SIMS (Caltech) (TP, YG), SIMS (Kochi) (KS, TU), EPMA (Caltech) (EMS, MB, CM), EPMA (AMNH) (YM, SD, WHT), visualisation and data compilation (YM), writing and interpretation: all authors, first draft (YM).

Scientific editing by Thomas C. Meisel.

Data availability statement

Raw FTIR spectra are archived as Moussallam (2024a). Raw NRA spectra are archived as Moussallam (2024b).

References

Albarède F. (2009)
Volatile accretion history of the terrestrial planets and dynamic implications. **Nature**, **461**, 1227–1233.

Allard P. (2010)
A CO_2-rich gas trigger of explosive paroxysms at Stromboli basaltic volcano, Italy. **Journal of Volcanology and Geothermal Research**, **189**, 363–374.

Allison C.M., Roggensack K. and Clarke A.B. (2019)
H_2O–CO_2 solubility in alkali-rich mafic magmas: New experiments at mid-crustal pressures. **Contributions to Mineralogy and Petrology**, **174**, 58, https://doi.org/10.1007/s00410-019-1592-4

Armstrong J. (1995)
CITZAF: A package of correction programs for the quantitative electron microbeam X-ray-analysis of thick polished materials, thin films, and particles. **Microbeam Analysis**, **4**, 177.

references

Armstrong J. and Crispin K. (2013)
Ultra-thin iridium as a replacement coating for carbon in high resolution quantitative analyses of insulating specimens. **Microscopy and Microanalysis**, 19, 1070–1071.

Befus K.S., Walowski K.J., Hervig R.L. and Cullen J.T. (2020)
Hydrogen isotope composition of a large silicic magma reservoir preserved in quartz-hosted glass inclusions of the Bishop Tuff plinian eruption. **Geochemistry, Geophysics, Geosystems**, 21, e2020GC009358.

Blank J.G. and Brooker R.A. (1994)
Experimental studies of carbon dioxide in silicate melts: Solubility, speciation, and stable carbon isotope behavior. **Reviews in Mineralogy and Geochemistry**, 30, 157–186.

Blank J.G. (1993)
An experimental investigation of the behavior of carbon dioxide in rhyolitic melt. PhD thesis, **California Institute of Technology**. https://doi.org/10.7907/tq3x-2059

Brooker R., Holloway J.R. and Hervig R. (1998)
Reduction in piston-cylinder experiments: The detection of carbon infiltration into platinum capsules. **American Mineralogist**, 83, 985–994.

Bureau H., Raepsaet C., Khodja H., Carraro A. and Aubaud C. (2009)
Determination of hydrogen content in geological samples using elastic recoil detection analysis (ERDA). **Geochimica et Cosmochimica Acta**, 73, 3311–3322.

Caulfield J., Turner S., Arculus R., Dale C., Jenner F., Pearce J. *et al.* (2012)
Mantle flow, volatiles, slab-surface temperatures and melting dynamics in the north Tonga arc–Lau back-arc basin. **Journal of Geophysical Research: Solid Earth**, 117, https://doi.org/10.1029/2012JB009526

Clesi V., Bouhifd M.A., Bolfan-Casanova N., Manthilake G., Schiavi F., Raepsaet C. *et al.* (2018)
Low hydrogen contents in the cores of terrestrial planets. **Science Advances**, 4, e1701876.

Dasgupta R. and Hirschmann M.M. (2006)
Melting in the Earth's deep upper mantle caused by carbon dioxide. **Nature**, 440, 659–662.

Dehant V., Debaille V., Dobos V., Gaillard F., Gillmann C., Goderis S. *et al.* (2019)
Geoscience for understanding habitability in the solar system and beyond. **Space Science Reviews**, 215, 42.

Dixon J.E., Stolper E. and Delaney J.R. (1988)
Infrared spectroscopic measurements of CO_2 and H_2O in Juan de Fuca Ridge basaltic glasses. **Earth and Planetary Science Letters**, 90, 87–104.

Edmonds M. and Woods A.W. (2018)
Exsolved volatiles in magma reservoirs. **Journal of Volcanology and Geothermal Research**, 368, 13–30.

Eggler D.H. (1976)
Does CO_2 cause partial melting in the low-velocity layer of the mantle? **Geology**, 4, 69–72.

Ehlmann B.L., Anderson F.S., Andrews-Hanna J., Catling D.C., Christensen P.R., Cohen B.A. *et al.* (2016)
The sustainability of habitability on terrestrial planets: Insights, questions, and needed measurements from Mars for understanding the evolution of Earth-like worlds. **Journal of Geophysical Research: Planets**, 121, 1927–1961.

Elskens I., Tazieff H. and Tonani F. (1968)
Investigations nouvelles sur les gaz volcaniques. **Bulletin Volcanologique**, 32, 521–574.

Foley B.J. and Smye A.J. (2018)
Carbon cycling and habitability of Earth-sized stagnant lid planets. **Astrobiology**, 18, 873–896.

Hammerli J., Hermann J., Tollan P. and Naab F. (2021)
Measuring *in situ* CO_2 and H_2O in apatite via ATR-FTIR. **Contributions to Mineralogy and Petrology**, 176, 105.

Hauri E., Wang J., Dixon J.E., King P.L., Mandeville C. and Newman S. (2002)
SIMS analysis of volatiles in silicate glasses: 1. Calibration, matrix effects and comparisons with FTIR. **Chemical Geology**, 183, 99–114.

Hervig R.L., Moore G.M. and Roggensack K. (2009)
Calibrating carbon measurements in basaltic glass using SIMS and FTIR: The effect of variable H_2O contents. **AGU Fall Meeting Abstracts**, V51E-1755.

Iacono-Marziano G., Morizet Y., Le Trong E. and Gaillard F. (2012)
New experimental data and semi-empirical parameterization of H_2O–CO_2 solubility in mafic melts. **Geochimica et Cosmochimica Acta**, 97, 1–23.

Jarosewich E., Nelen J.A. and Norberg J.A. (1980)
Reference samples for electron microprobe analysis. **Geostandards Newsletter**, 4, 43–47.

Jochum K.P., Stoll B., Herwig K., Willbold M., Hofmann A.W., Amini M. *et al.* (2006)
MPI-DING reference glasses for *in situ* microanalysis: New reference values for element concentrations and isotope ratios. **Geochemistry, Geophysics, Geosystems**, 7, https://doi.org/10.1029/2005GC001060.

Joesten R.L. (1974)
Metasomatism and magmatic assimilation at a gabbro-limestone contact, Christmas Mountains, Big Bend region, Texas. **PhD thesis, California Institute of Technology.** https://resolver.caltech.edu/CaltechTHESIS:02272014-085454874

Kamenetsky V.S., Everard J.L., Crawford A.J., Varne R., Eggins S.M. and Lanyon R. (2000)
Enriched end-member of primitive MORB melts: Petrology and geochemistry of glasses from Macquarie Island (SW Pacific). **Journal of Petrology**, 41, 411–430.

Keller N.S., Arculus R.J., Hermann J. and Richards S. (2008)
Submarine back-arc lava with arc signature: Fonualei Spreading Center, northeast Lau Basin, Tonga. **Journal of Geophysical Research: Solid Earth**, 113, B08S07.

references

Khodja H., Berthoumieux E., Daudin L. and Gallien J.-P. (2001)
The Pierre Süe Laboratory nuclear microprobe as a multi-disciplinary analysis tool. Nuclear Instruments and Methods in Physics Research Section B, 181, 83–86.

Krzhizhanovskaya M.G., Chukanov N.V., Mazur A.S., Pautov L.A., Varlamov D.A. and Bocharov V.N. (2023)
Crystal chemistry and thermal behavior of B-, S- and Na-bearing spurrite. Physics and Chemistry of Minerals, 50, 33.

Lesne P., Scaillet B., Pichavant M. and Beny J.-M. (2011)
The carbon dioxide solubility in alkali basalts: An experimental study. Contributions to Mineralogy and Petrology, 162, 153–168.

Lloyd A.S., Plank T., Ruprecht P., Hauri E.H. and Rose W. (2013)
Volatile loss from melt inclusions in pyroclasts of differing sizes. Contributions to Mineralogy and Petrology, 165, 129–153.

Malavergne V., Bureau H., Raepsaet C., Gaillard F., Poncet M., Surblé S. *et al.* (2019)
Experimental constraints on the fate of H and C during planetary core-mantle differentiation. Implications for the Earth. Icarus, 321, 473–485.

Mayer M. (1999)
SIMNRA – A simulation program for the analysis of NRA, RBS and ERDA. AIP Conference Proceedings, 475, 541–544.

Métrich N. and Wallace P.J. (2008)
Volatile abundances in basaltic magmas and their degassing paths tracked by melt inclusions. Reviews in Mineralogy and Geochemistry, 69, 363–402.

Mosbah M., Metrich N. and Massiot P. (1991)
PIGME fluorine determination using a nuclear microprobe with application to glass inclusions. Nuclear Instruments and Methods in Physics Research Section B, 58, 227–231.

Moussallam Y. (2024a)
ND70 paper_Raw FTIR spectra [Data set]. Figshare, https://doi.org/10.6084/m9.figshare.25292692.v1

Moussallam Y. (2024b)
ND70 paper_Raw NRA Spectra [Data set]. Figshare, https://doi.org/10.6084/m9.figshare.25292674.v1

Moussallam Y., Morizet Y., Massuyeau M., Laumonier M. and Gaillard F. (2015)
CO_2 solubility in kimberlite melts. Chemical Geology, 418, 198–205.

Moussallam Y., Oppenheimer C., Scaillet B., Buisman I., Kimball C., Dunbar N. *et al.* (2015)
Megacrystals track magma convection between reservoir and surface. Earth and Planetary Science Letters, 413, 1–12.

Moussallam Y., Morizet Y. and Gaillard F. (2016)
H_2O–CO_2 solubility in low SiO_2-melts and the unique mode of kimberlite degassing and emplacement. Earth and Planetary Science Letters, 447, 151–160.

Moussallam Y., Lee H.J., Ding S., DeLessio M., Everard J.L., Spittle E. *et al.* (2023)
Temperature of the Villarrica Lava Lake from 1963 to 2015 constrained by phase-equilibrium and a new glass geothermometer for basaltic andesites. Journal of Petrology, 64, https://doi.org/10.1093/petrology/egad003

Nicoli G. and Ferrero S. (2021)
Nanorocks, volatiles and plate tectonics. Geoscience Frontiers, 12, 101188.

Shi S.C., Towbin W.H., Plank T., Barth A., Rasmussen D., Moussallam Y. *et al.* (2023)
PyIRoGlass: An open-source, Bayesian MCMC algorithm for fitting baselines to FTIR spectra of basaltic-andesitic glasses. https://eartharxiv.org/repository/view/6193/

Shimizu K., Saal A.E., Hauri E.H., Perfit M.R. and Hékinian R. (2019)
Evaluating the roles of melt-rock interaction and partial degassing on the CO_2/Ba ratios of MORB: Implications for the CO_2 budget in the Earth's depleted upper mantle. Geochimica et Cosmochimica Acta, 260, 29–48.

Shimizu K., Suzuki K., Saitoh M., Konno U., Kawagucci S. and Ueno Y. (2015)
Simultaneous determinations of fluorine, chlorine, and sulfur in rock samples by ion chromatography combined with pyrohydrolysis. Geochemical Journal, 49, 113–124.

Shimizu K., Ushikubo T., Hamada M., Itoh S., Higashi Y., Takahashi E. and Ito M. (2017)
H_2O, CO_2, F, S, Cl, and P_2O_5 analyses of silicate glasses using SIMS: Report of volatile standard glasses. Geochemical Journal, 51, 299–313.

Shishkina T.A., Botcharnikov R.E., Holtz F., Almeev R.R. and Portnyagin M.V. (2010)
Solubility of H_2O- and CO_2-bearing fluids in tholeiitic basalts at pressures up to 500 MPa. Chemical Geology, 277, 115–125.

Stern R.J. (2018)
The evolution of plate tectonics. Philosophical Transactions of the Royal Society A, 376, 20170406.

Stolper E. and Holloway J.R. (1988)
Experimental determination of the solubility of carbon dioxide in molten basalt at low pressure. Earth and Planetary Science Letters, 87, 397–408.

Tamic N., Behrens H. and Holtz F. (2001)
The solubility of H_2O and CO_2 in rhyolitic melts in equilibrium with a mixed CO_2-H_2O fluid phase. Chemical Geology, 174, 333–347.

Webster J.D., Goldoff B. and Shimizu N. (2011)
C–O–H–S fluids and granitic magma: How S partitions and modifies CO_2 concentrations of fluid-saturated felsic melt at 200 MPa. **Contributions to Mineralogy and Petrology, 162**, 849–865.

Wyllie P.J. (1971)
Role of water in magma generation and initiation of diapiric uprise in the mantle. **Journal of Geophysical Research, 76**, 1328–1338.

Supporting information

The following supporting information may be found in the online version of this article:

Figure S1. Elemental analyser secondary calibration.

Figure S2. $^{16}O^{1}H$ signal retrieved by SIMS using a Cs^+ primary beam at the Nancy, Kochi, WHOI and Caltech ion probe facilities.

Figure S3. ^{12}C signal retrieved by SIMS using a Cs^+ primary beam at the Nancy, Kochi, WHOI and Caltech ion probe facilities.

Figure S4. ^{32}S signal retrieved by SIMS using a Cs^+ primary beam at the Nancy, Kochi, WHOI and Caltech ion probe facilities.

Figure S5. ^{35}Cl signal retrieved by SIMS using a Cs^+ primary beam at the Nancy, Kochi, WHOI and Caltech ion probe facilities.

Figure S6. ^{19}F signal retrieved by SIMS using a Cs^+ primary beam at the Nancy, Kochi, WHOI and Caltech ion probe facilities.

Figure S7. Signal retrieved by SIMS using a O^- primary beam at WHOI and Caltech Ion Probe facilities.

Figure S8. Plot of measurement results for CO_2 by EPMA vs. accepted CO_2 values for secondary reference materials.

Figure S9. FTIR spectra of ND70 series glasses and spectra fitting with the PyIRoGlass software (Shi *et al.* 2023).

Table S1. Mass of all starting materials added to each experiment.

Table S2. Volatile and SiO_2 contents of other glasses analysed.

Table S3. Raw SIMS measurement results from IMS 1280 at CNRS-CRPG Nancy using a Cs^+ primary beam.

Table S4. Raw SIMS measurement results from IMS 7f-GEO at Caltech using a Cs^+ primary beam.

Table S5. Raw SIMS measurement results from IMS 1280 at WHOI using a Cs^+ primary beam.

Table S6. Raw SIMS measurement results from IMS 7f-GEO at Caltech using a O^- primary beam.

Table S7. Raw SIMS measurement results from IMS 1280 at WHOI using a O^- primary beam.

Table S8. Raw SIMS measurement results from IMS 1280 at JAMSTEC Kochi Institute using a Cs^+ primary beam.

Table S9. Data used to generate Figure 8.

This material is available from: http://onlinelibrary.wiley.com/doi/10.1111/ggr.12572/abstract (This link will take you to the article abstract).